

Detection of Trigger Events for Successful Investments: Non-Parametric Analysis of Real Options with Early Exercise

Cedric Y. Justin¹ and Dimitri N. Mavris²
Georgia Institute of Technology, Atlanta, Georgia

In a symposium held at Georgetown University in 2003, a panel of academics and practitioners identified a set of requirements known as the *Georgetown Challenge* that real option analyses must meet in order to get more traction and wider acceptance amongst practitioners in the industry. In a bid to meet some of these challenges, this research proposes a non-parametric approach for the evaluation of real options featuring early-exercise possibilities. It features a real option analysis framework aimed at substantiating decision making for research and development investments while having a wider domain of application and an improved ability to handle a complex reality compared to typical approaches suggested in textbooks. It cross-fertilizes techniques used in actuarial sciences, in statistics, and in finance to yield a transparent methodology articulated around four steps easily applicable by practitioners. First, it uses (Quasi-) Monte Carlo techniques to simulate the evolution of market uncertainties driving the value of real options embedded in investments. Then, a non-parametric Esscher transform is implemented to achieve a change of probability measure to obtain, at each time step in the simulation, a weighted distribution representing the investment value under the equivalent martingale measure. Next, it applies a bootstrap technique to resample these weighted distributions so as to construct new non-weighted trajectories representing the evolution of the investment value under the equivalent martingale measure. Finally, a regression-based technique is used to value real options with early-exercise possibilities: the optimum trigger boundary is first determined and the embedded real options are priced next. Several improvements to the regression-based technique are proposed to significantly improve the accuracy of the trigger boundary, and in particular, the use of a multi-start (quasi-) Monte Carlo simulation is suggested. Verification is performed on canonical examples and indicate good accuracy and competitive execution time.

JEL classification: G13, G31, C63, O32

Keywords: Real-options, Early-exercise boundary, Esscher transform, Simulation, Bootstrapping

1 Introduction

Graham and Harvey [1] report that discounted cash flow analyses are traditionally used to assess the economic performance of investments. This type of analyses is however not well suited for projects subject to uncertainty, projects with staggered investments, and projects with cash inflows occurring long after the initial investments. Typical examples of such projects include research and development programs for which the use of discounted cash flow analyses may lead to an incorrect valuation and a possible rejection of profitable projects. Part of this problem lays in the fact that discounted cash flow analyses are deterministic and therefore do not handle well projects spanning over multiple years, featuring several decision tollgates, and riddled with uncertainties. One method to assess project viability under uncertainty features real options [2]. Real option analysis is an emerging field in corporate finance [3] where it is used to substantiate capital budgeting decisions. It is derived from the

¹ PhD Candidate, e-mail: cedric.justin@gatech.edu

² Boeing Regents Professor of Advanced Aerospace Systems, e-mail: dimitri.mavris@aerospace.gatech.edu

financial option analysis pioneered with the seminal work of Black, Scholes, [4] and Merton [5]. Real option analysis may be interpreted as an extension of the discounted cash flow analysis in that it uses the concept of time-value of money but goes beyond and recognizes the fact that managers react to changes in the business environment and actively steer projects into profitable directions. Consequently, a real option approach accounts for the flexibility offered to management to abandon unprofitable programs.

There is little doubt that real option inspired methodologies present an attractive concept for capital allocation budgeting problems due to their abilities to better mimic the decision processes that take place within companies as uncertainty unfolds. For instance, Shackleton et al. [6] use real options to analyze R&D programs in the aerospace industry. However, as much as option-thinking seems promising for analyzing investments featuring flexibility, the implementation and adoption of real options within companies have been slow [7]. There may be several reasons to this and one of them may be the complexity of developing a relevant real option framework. While simpler models using the closed-form Black-Scholes formula have been attractive initially due to their simplicity, their validity for corporate investment valuation may be questionable. Some of the assumptions underpinning the Black-Scholes model are quite strong and may not be appropriate for corporate investments [8]. More generic methods using Monte Carlo simulations have been proposed over the years and relax some of these assumptions but the explicit formulation of a model for the evolution of the business prospect value remains problematic. Even though analysts may have access to a lot of real data and may be able to model the evolution of one or more sources of uncertainty over time, when several sources of uncertainty impact a development program, fitting a model to simulate the stochastic evolution of the development program value becomes significantly harder.

In a symposium held at Georgetown University in 2003, a panel of academics and practitioners identified a set of requirements known as the *Georgetown Challenge* [9] that real option analyses must meet in order to get more traction and get wider acceptance amongst practitioners in the industry. These requirements revolve around seven points summarized in Table 1. A real option methodology has to dominate other capital budgeting techniques by recognizing the flexibility offered to decision makers and the resulting value created by active and astute management. It has to capture the reality of the problem by being flexible enough to handle the idiosyncrasies of investments. For instance, investments are typically not decided at pre-determined dates but can be decided whenever conditions become optimal. The methodology has to use mathematics that everyone can understand in order to avoid the “black-box” type of issues it currently faces. It has to rule out the possibility of mispricing by eliminating arbitrage and has to be empirically testable. It must incorporate risk appropriately by handling differently the idiosyncratic and market risks, which means that for R&D programs, technical risk must be handled differently. Finally, real option analyses must use as much market information as possible to remove as much subjectivity as possible.

Table 1: Identification of challenges for successful implementation of real option analyses

Georgetown Challenge Requirements (Adapted from Copeland and Antikarov [9])	Intuitively dominate other decision-making methods
	Capture the reality of the problem
	Use mathematics that everyone can understand
	Rule out the possibility of mispricing by eliminating arbitrage
	Be empirically testable
	Appropriately incorporate risk
	Use as much market information as possible

A significant issue faced by many real option practitioners is the inability of simpler real option techniques to accurately capture the reality of the problem. This issue is broad and may range from the overwhelming use of geometric Brownian motion as *the* stochastic process in many textbooks, to the inability of many techniques to handle multiple correlated uncertainties, and finally, to the inability of many techniques to properly handle options featuring early-exercise possibilities. One objective of this research is to provide a generic framework that better captures the reality of the problem and therefore overcomes the aforementioned challenges. In particular, decision-makers usually need not wait until a pre-specified date to make a decision: instead, they make investment decisions whenever the situation is right and the likelihood of success is greatest. One requirement for the proposed methodology is thus its suitability for the analysis of real options that can be exercised at any given point in time before expiration (American or Bermudan real options). Another objective of this research is to help managers make optimal investment choices: in competitive scenarios, the timing of investments is paramount and the identification of the optimal timing of investments becomes very relevant. This research therefore puts significant emphasis on the construction of the early-exercise boundary or trigger boundary. The trigger boundary is defined by the set of external conditions (time and state of uncertainties) that makes investing early optimal. It is relevant to decision-makers as it allows them to substantiate whether acting now or delaying the exercise of the option is optimal: by comparing the current state of the business to the trigger boundary, decision-makers are able to identify whether the current situation is within an invest-immediately area or whether it is within a wait-and-see area and more value is obtained by holding the real option. Any time an investment is made prior to the latest time at which investment decisions can possibly be made, the decision is called an early investment decision. The investment policy is defined as the policy of timing investments optimally which means that the policy maximizes value for the company. The policy determines the trigger boundary and investigating its shape may help answer the following questions:

- *Which uncertainties affect most the trigger boundary?*
- *Which combinations of uncertainties and their respective levels induce trigger events?*
- *How does the erosion of competitive advantages affect the trigger boundary?*
- *How much time remains before the company can be expected to hit the trigger boundary?*

In this context, the current research proposes a new transparent and integrated methodology aimed at helping decision-makers investigate the viability of investments and optimize their timing. This value-driven methodology is the foundation for a strategic decision-making framework that facilitates the formulation of robust and competitive solutions through the identification of trigger events or sets of market conditions that make investing optimal. This research cross-fertilizes techniques used in finance, statistics, and actuarial sciences to yield a methodology that features several improvements over traditional methods: a bootstrapping technique is used to both incorporate as much market data as possible and resample the evolution of the underlying business venture under the equivalent martingale measure; a non-parametric Esscher transform is applied to perform a change of probability measure for the evolution of the business venture value; and finally, regression-based techniques are implemented to both value real options with early-exercise possibilities and determine optimal investment timing. Several improvements to popular regression-based Monte Carlo algorithms are implemented and a new multi-start (Quasi-) Monte Carlo simulation approach is suggested to improve the accuracy of the trigger boundary construction.

2 Proposed Methodology for Real Options with Early Investment Flexibility

In the preceding sections, real option analysis has been introduced as a means to analyze research and development programs subject to uncertainties and featuring decision tollgates. In this section, the paper proposes a new methodology for the analysis of real options. The methodology aims at remaining as generic as possible – even

non-parametric in some sense – so that it can be used and adapted to many types of investments featuring managerial flexibility. Another aim of this methodology is to use techniques widely accepted within companies so that real option analyses become more accessible to practitioners. The proposed methodology is articulated around four steps which are reviewed individually in the subsequent paragraphs. The first step consists in modeling and simulating the uncertainties impacting the value of the development program. This modeling is achieved using potentially correlated stochastic processes which are then simulated with (Quasi-) Monte Carlo simulation. At each time step in the simulation, the value of the business prospect is derived using deterministic parameters as well as a state vector representing the realization of the uncertainties. In a second step, the stochastic process representing the value of the business prospect is transformed and expressed in the equivalent martingale measure using the non-parametric Esscher transform. In the third step, bootstrapping is used to resample the (weighted) distribution under the new martingale measure so as to construct non-weighted trajectories representing the evolution of the business prospect value. Finally, in the last step, a regression-based technique is used to approximate the trigger boundary and estimate the value of the real option with early exercise possibilities.

2.1 Uncertainty modeling

In this step, market uncertainties that have the most impact on the value of the business prospect are first identified. These uncertainties are then simulated to generate possible trajectories for the project value over time. The simulation can be achieved in two different manners, either parametrically or non-parametrically. If the analyst is presented with sufficient market information and feels that fitting a model is adequate, a stochastic process is calibrated and (Quasi-) Monte Carlo simulations are then used to represent the evolution of the uncertainty under the physical probability measure. If there is a substantial risk of model misspecification, an alternative and non-parametric simulation is achieved by resampling data derived from the market, which in some sense removes as much subjectivity as possible. The resampling is achieved using a bootstrap technique.

2.1.1 Using (Quasi-) Monte Carlo simulations

Market uncertainties are modeled with stochastic processes and calibrated using data derived from the market to remove subjectivity and prevent the possibility of arbitrage in the valuation. Using these stochastic processes, (Quasi-) Monte Carlo simulations are performed. This leads to a state vector representing the realization of each uncertainty at each time step in the simulation. If uncertainties are correlated, the correlations are accounted for using correlated random numbers. Cholesky decomposition can be used to generate correlated random numbers for this purpose. A business model calculator is used next as a “transfer function” representing the value of the business prospect under review given the state of the uncertainties. This process is illustrated in Figure 1.

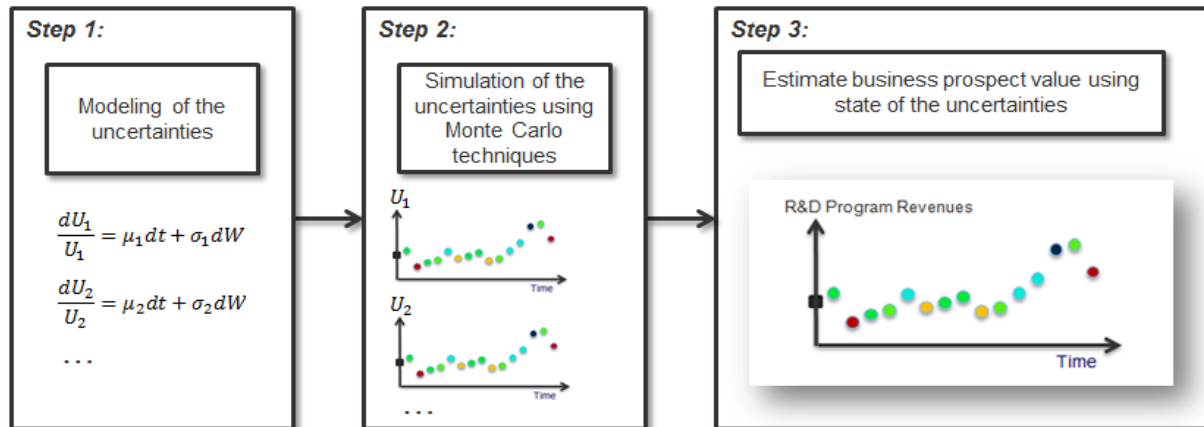


Figure 1: Uncertainty modeling and Monte Carlo simulations under the physical probability measure

The process is then repeated many times to end up with a distribution (sample) of business prospect values at each time step in the simulation. The evolution of the business prospect value is simulated under the physical or historical probability measure since the models used for the evolution of the uncertainties are calibrated using observations from the market.

2.1.2 Using resampling techniques

There might be cases for which a proper calibration of the stochastic process to the data is challenging. This is true for complex stochastic behaviors for which high frequency market data must be available such as when jumps or discontinuities occur. In these cases, resampling techniques which consist in sampling directly from observed data may be used. Bootstrapping is a popular statistical method whose name was first coined by Efron in his 1979 Rietz Lecture [10] to describe a resampling technique used to estimate the precision of some statistics such as the mean, median, or standard deviation of a distribution. In the original application, bootstrap samples were constructed by sampling with replacement a subset of an original distribution and statistics of interest were then computed. For the simulation of uncertainties, the essence of the bootstrap method is retained but the application is different: similarly, the bootstrap method is used to sample with replacement from an original distribution (empirical sample) but what is new is that the bootstrap sample is used next to generate trajectories representing the evolution of uncertainties. Like in the Monte Carlo simulation approach, a business model calculator is used next as a “transfer function” representing the value of the business prospect given the state of the uncertainties at each time step in the simulation. This yields trajectories representing the evolution of the business prospect value over time as shown in Figure 2.

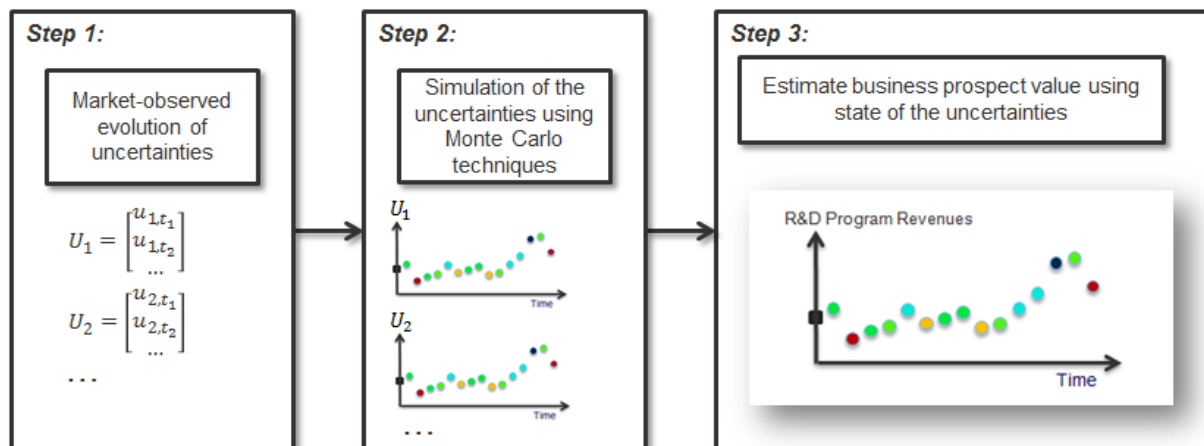


Figure 2: Resampling with bootstrap method

2.2 Change of probability measure with Esscher transform and its non-parametric approximation

For option valuation purposes, the dynamics of the business prospect value must be specified using the equivalent martingale measure or equivalent risk-neutral probability measure. This enables the computation of the present value of the real option through a discounting of the payoffs using the risk-free rate of return. A change of probability measure is therefore required. The equivalent martingale measure is a probability measure for which the returns of all assets are exactly the risk-free rate of return. Mathematically, this is equivalent to subtracting the risk-premium from the expected returns which makes investors indifferent towards risk, hence the name of the measure.

2.2.1 Using Esscher transform

A change of probability measure technique was proposed in 1994 by Gerber and Shiu [11] to handle a wide variety of processes featuring stationary and independent increments such as Wiener processes, Poisson processes, Gamma processes, and inverse Gaussian processes. A transformation based on the Esscher transform [12], a time-

honored tool in actuarial finance pioneered by Swedish mathematician Fredrik Esscher and publicized by Kahn [13], is used to induce an equivalent probability measure. For a probability density function f and a real number h , the Esscher transform f_{Ess} with parameter h is expressed using M the moment generating function of f shown in Eq. 1:

$$f_{Ess}(x, h) = \frac{e^{hx}f(x)}{M(h)}, \text{ with } h \in \mathbb{R} \text{ and } M(h) = \int_{-\infty}^{\infty} e^{hx}f(x)dx \quad \text{Eq. 1}$$

Looking at this definition, the Esscher transform is the product of an exponential function and a density function, normalized by a moment generating function. As a result, this transformation induces an equivalent probability measure as both distributions agree on sets with probability zero. It also becomes clear why the Esscher transform is sometimes called exponential tilting: the transformation distorts the original probability measure using an exponential function. The aim of Gerber and Shiu is to use the free parameter h introduced by the Esscher transform to ensure that the new probability measure is an equivalent martingale measure. In other terms, the parameter h is determined to ensure that the discounted business prospect value is a martingale which means that the value of the underlying business prospect is exactly its expected discounted payoff. When markets are complete, the equivalent martingale measure is unique and therefore the Esscher transform yields the unique arbitrage-free price for the real option. The marketed asset disclaimer assumption [14] ensures that the market is complete and therefore that a unique price for the real option can be found. On the other hand, when the market is incomplete, the claim is not attainable and there is no possibility for the market and its arbitrageurs to *enforce* a no-arbitrage price. Mathematically, there may be many equivalent martingale measures and the practitioner has to select one of them. Several equivalent measures [15] have been proposed such as the minimal martingale measure [16], the minimal entropy martingale measure [17], the utility martingale measure [17], and of course, the Esscher martingale measure. Each of them corresponds to a different attitude towards risk and consequently some assumptions regarding the preferences and risk attitude of decision-makers must be set to pick which utility function and therefore which equivalent martingale measure is most appropriate. In fact, in the discussion pertaining to their paper [18], Gerber and Shiu show that the Esscher martingale measure is consistent with investors or decision-makers exhibiting power utility behaviors³. Power utility functions, also known as iso-elastic utility functions, have the property of constant relative risk aversion which means that the risk aversion is independent of the level of initial wealth. The power utility assumption has the advantage of being consistent with some other fundamental results of finance and economics (mutual fund theorem in Cass and Stiglitz [19] and Stiglitz [20] for instance). Surprisingly, the Esscher transformation has never been used for real option analysis to the authors' knowledge.

2.2.2 Using the non-parametric approximation of the Esscher transform

A significant hurdle is that the Esscher transform as introduced above requires an explicit formulation for the probability density function f representing the distribution of the business prospect value at a given point in time. While it may be known to the practitioner in some simple cases, most of the times analysts have little or no information as to the distribution of the business prospect value once all uncertainties are mixed in the business prospect value computation. In fact, one major objective of this research is to enable option valuation without the need to specify a parametric model (i.e. time-indexed distributions) for the underlying business prospect value because of the high subjectivity involved when selecting models that are not directly observable in the market.

³ A power utility function belongs to the class of hyperbolic absolute risk aversion utility functions. It is a special case in that it exhibits a constant relative risk aversion. The power utility function relates the utility U to the level of consumption c using the following formula with η a constant measuring risk-aversion:

$$U(c) = \begin{cases} \frac{c^{1-\eta}-1}{1-\eta} & \eta > 0, \eta \neq 1 \\ \ln(c) & \eta = 1 \end{cases}$$

Adapting the Esscher transformation technique so that it does not require the explicit formulation of the underlying stochastic process (and its associated distribution at each time step) would prove particularly useful for real option analysis. Pereira, Epprecht, and Veiga [21] propose a model-free, non-parametric approximation of the Esscher transform presented previously to transform the behavior of an underlying asset from the physical probability measure to the equivalent martingale measure. The technique is geared towards the pricing of financial options and needs to be adapted for the economic evaluation of corporate investments featuring flexibility.

The first step of the non-parametric Esscher transformation starts with the collection of the n business prospect values $S_t^{j=1..n}$ at a given time cross-section t . This data may have either one of two origins: it can be directly observable and available (such as the market price of the underlying asset) or it can be generated by the practitioner if the underlying asset is synthetic and not publicly traded. These values are used to estimate the n continuously compounded rates of return $x_t^{j=1..n}$ of the business prospect value. Let's now call \widehat{X}_t the vector of size n containing these n rates of return from the (unknown) business prospect return distribution at time t as shown in Eq. 2:

$$\widehat{X}_t = [x_t^1, x_t^2, x_t^3 \dots x_t^n] = \left[\ln\left(\frac{S_t^1}{S_{t-1}^1}\right), \ln\left(\frac{S_t^2}{S_{t-1}^2}\right), \ln\left(\frac{S_t^3}{S_{t-1}^3}\right) \dots \ln\left(\frac{S_t^n}{S_{t-1}^n}\right) \right] \quad \text{Eq. 2}$$

The second step consists in the computation of the empirical moment generating function which is estimated using Eq. 3:

$$\widehat{M}_t(h, t) = \frac{1}{n} \sum_{i=1}^n e^{hx_t^i} \quad \text{Eq. 3}$$

The third step is directly inspired by the work of Gerber and Shiu in that it solves for the specific value of the parameter h such that the asset price is a martingale under the new probability measure. This specific parameter value, denoted h^* , solves Eq. 4 and in a complete market with no arbitrage, the fundamental theorem of asset pricing [22] ensures that this solution is unique.

$$e^{rf} = \frac{\sum_{i=1}^n e^{(h^*+1)x_t^i}}{\sum_{i=1}^n e^{h^*x_t^i}} \quad \text{Eq. 4}$$

With the proper value h^* of the Esscher transform parameter, the final step consists in constructing the new probability measure. This is done by reweighting each observation and ensuring that their probabilities sum to one. The new probability vector giving the probability of each observation under the new measure is given by Eq. 5. This is the set of probabilities that is used for the pricing of options and for the computation of expectations.

$$\mathbb{Q}_t^{h^*} = \left[\frac{e^{h^*x_t^1}}{\sum_{i=1}^n e^{h^*x_t^i}}, \frac{e^{h^*x_t^2}}{\sum_{i=1}^n e^{h^*x_t^i}}, \dots, \frac{e^{h^*x_t^n}}{\sum_{i=1}^n e^{h^*x_t^i}} \right] \quad \text{Eq. 5}$$

In summary, the non-parametric Esscher transform enables practitioners to distort an unknown probability distribution into a risk-neutral probability distribution. This transformation is done at each time cross-section in the simulation and consists of weighting each observation in the cross-section sample. This weighted sample of returns is converted back to business prospect values and subsequently used to estimate the expected option payoff which is discounted to the present time using the risk-free interest rate. Provided mild conditions of stationarity and increment independence are satisfied, the non-parametric Esscher transform tremendously simplifies the analyses of practitioners who no longer need to calibrate and substantiate the choice of one particular stochastic process for the

usually unknown evolution of the business prospect value. The algorithm to perform the change of measure is depicted in Figure 3.

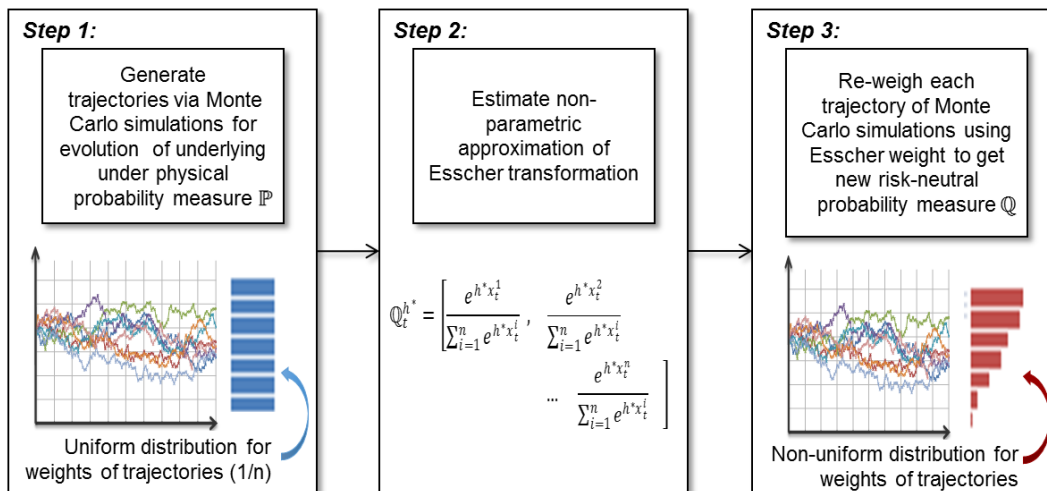


Figure 3: Non-parametric Esscher transform for change of probability measure

2.3 Resampling using the bootstrap technique

The non-parametric Esscher transform enables a change of probability measure and the expression of the evolution of the business prospect value under the equivalent martingale measure, a necessary step for option pricing using simulation. The technique changes the mean of the business prospect value distribution at each intermediate step by reweighting the different outcomes. In other words, the procedure described so far yields different sets of weights at each intermediate time step in the simulation. Thus, a given trajectory is made of time-indexed observations that have different weights attached to each observation. As much as the procedure is suitable for valuing European options for which the weighting may be performed just once at expiration when payoffs are computed, valuing American or Bermudan options is more difficult since it requires identically weighted observations at each time cross-section on a trajectory (to perform regressions as will be explained in 2.4).

With this issue in mind, we propose a way forward using a resampling technique while still assuming a stationary process with independent increments for the evolution of the business prospect value. A single time cross-section of weighted business prospect returns obtained from the non-parametric Esscher transformation is first selected. Alternatively, several time cross-sections may be pooled together in order to increase the size of the pooled sample of returns. The bootstrap technique described previously is then applied to this sample of weighted returns and consists in repetitive sampling with replacement to generate a new non-weighted sample of returns. Nevertheless, the weights (or probabilities) associated with each return in the original sample have to be accounted for when sampling with replacement to ensure that the properties of the equivalent martingale measure are preserved and carried over to the new trajectories being generated.

This is done by figuratively stacking all the weights in one column, the “height” of which is one since the weights represent a probability measure. Next, a random number is drawn from a uniform distribution (between zero and one) to define which level in the column is reached and therefore which piece of the stack is selected. The selected piece corresponds to a return which is then used to construct a new trajectory as illustrated in Figure 4. In doing so, returns with larger weights (probabilities) have a greater chance of being drawn while returns with smaller weights (probabilities) have less chance of being drawn during the resampling effort. Starting with an initial

business prospect value, the resampling of returns enables the construction of trajectories representing the evolution of the business prospect value under the new equivalent martingale measure.

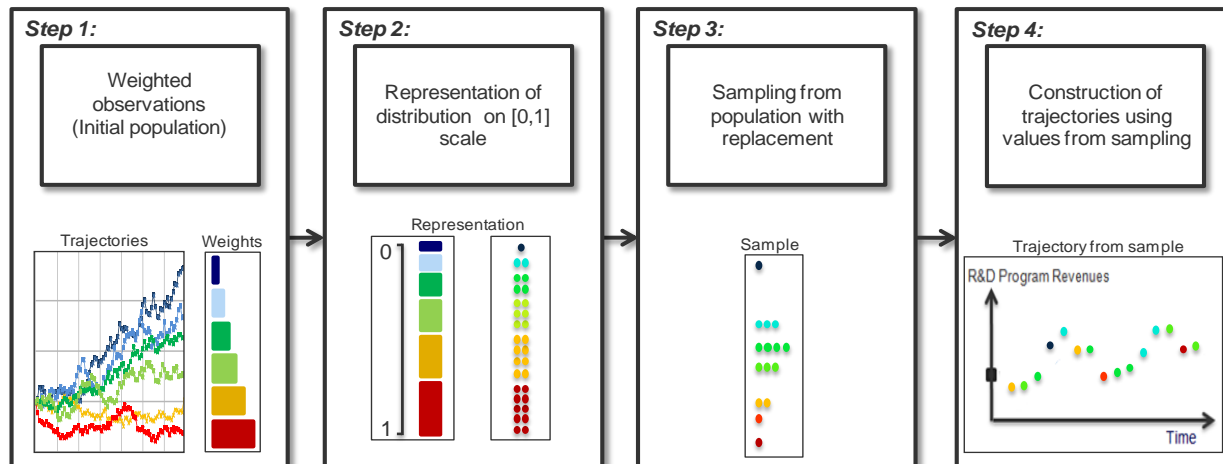


Figure 4: Bootstrapping weighted observations by first stacking weights and then sampling randomly from the stack (mapping between position in the stack and return value is known)

2.4 American option valuation and construction of the trigger boundary

This step is articulated around two objectives: the first consists in identifying when and under which circumstances it becomes optimal to invest in a business prospect featuring managerial flexibility, while the other consists in assessing the value of the real option.

2.4.1 Using least-squares Monte Carlo technique

For real option applications, Monte Carlo simulations enable the capture of a multitude of uncertainties and their interdependencies. However, pricing real options using Monte Carlo simulations has long been hindered by the perceived inability of simulation techniques to correctly handle path-dependent options [23]. Indeed, the value of the American option at the k^{th} time step t_k denoted V_{t_k} on an asset S with observed value S_{t_k} and with payoff function P can be expressed as the maximum between exercising immediately and holding the option as shown in Eq. 6. In other words, while marching forward in time, one has to compare the payoff earned from immediate exercise to the value of holding the option for at least one extra step. However, at time t_k there is yet no estimate of the present value of the one-period-ahead option value $V_{t_{k+1}}$.

$$V_{t_k} = \max[P(S_{t_k}), e^{-r_f(t_{k+1}-t_k)} E_{\mathbb{Q}}(V_{t_{k+1}} | S_{t_k})] \quad \text{Eq. 6}$$

Fortunately, this paradigm has evolved starting in 1993 with the paper of Tilley [24] which aims was to dispel the belief that American-style options could not be valued using simulations. A significant improvement came in 1996 with the work of Carriere [25] regarding the valuation of options with early-exercise properties. Faced with the same problem of estimating the one-period-ahead option value for subsequent comparison with the immediate exercise payoff, Carriere suggests the use of non-parametric regressions to regress the conditional expectation and therefore to estimate the value of holding the options. As noted by Stentoft [26], the reason for this regression is that a conditional expectation is a function and “*any function belonging to a separable Hilbert space may be represented as a countable linear combination of basis-functions for the space.*” Consequently, let’s introduce $\{\phi_i\}_1^\infty$ as a family of basis-functions for that space. The expectation may be rewritten and approximated using the first M basis-functions $\{\phi_i\}_{i=1}^M$ as shown in Eq. 7:

$$E_{\mathbb{Q}}(V_{t_{k+1}}|S_{t_k}) = \sum_{i=1}^{\infty} \alpha_i(t_k) \cdot \phi_i(S_{t_k}) \sim \sum_{i=1}^M \alpha_i(t_k) \cdot \phi_i(S_{t_k}) \quad \text{Eq. 7}$$

Any family of basis-functions should work but Carriere suggests using either splines or a polynomial smoother. Next task is the estimation of the coefficients α_i of the linear combination. This is done marching backward, starting at expiration and moving back until the present time: at expiration, the value of the option is exactly the payoff, while for all preceding time steps denoted t_k a regression is performed using the observations of the underlying value for the n simulated trajectories denoted $S_{t_k}^{j=1..n}$ as well as the continuation value $V_{t_{k+1}}^{j=1..n}$ (a conditional expectation). The regression objective is to select a family of coefficients $\{\alpha_i\}_1^M$ that minimizes the error between the regressed conditional expectations and the option values across the n simulated trajectories. This error is defined in Eq. 8:

$$\min_{\{\alpha_i\}_0^M} \sum_{j=1}^n \left(\sum_{i=1}^M \alpha_i(t_k) \cdot \phi_i(S_{t_k}^j) - V_{t_{k+1}}^j \right)^2 \quad \text{Eq. 8}$$

The immediate exercise value at time t_k denoted $P(S_{t_k})$ is compared next to the discounted regressed conditional expectation to find the option value defined in Eq. 9. The procedure is repeated for each trajectory at each time step marching back until the present time to find the value of the American option.

$$V_{t_k} = \max \left[P(S_{t_k}), e^{-r_f(t_{k+1}-t_k)} \sum_{i=1}^M \alpha_i(t_k) \cdot \phi_i(S_{t_k}) \right] \quad \text{Eq. 9}$$

The algorithm for American option valuation using simulation and regression techniques is depicted in Figure 5. A popular enhancement to this work is the least-squares Monte Carlo approach of Longstaff and Schwartz [27]. Dating back to 2001, this approach is very similar to the method of Carriere except for two facts: the algorithm uses a least-squares regression and the regression is made using only in-the-money paths. In the Longstaff-Schwartz method, the proposed regression uses an ordinary least-squares technique to regress the conditional expectation $E_{\mathbb{Q}}(V_{t_{k+1}}|S_{t_k})$ against a set of explanatory variables. The set of explanatory variables is a family of basis-functions denoted $\{\phi_i\}_1^M$ and valued using the conditioning underlying asset price S_{t_k} . One may use a simple monomial family $\{\phi_i: X \rightarrow X^{i-1}\}_{i=1}^M$ as the family of basis-functions, or some families of orthogonal polynomials such as the Chebyshev polynomials, the Legendre polynomials, and the Laguerre polynomials. Furthermore, the regression is performed using only paths that are in-the-money since the decision to exercise or not the option is only relevant whenever the option is in-the-money. According to Longstaff and Schwartz, “*by focusing on the in-the-money paths, [... this...] limits the region over which the conditional expectation must be estimated, and far fewer basis functions are needed to obtain an accurate approximation to the conditional expectation function.*”

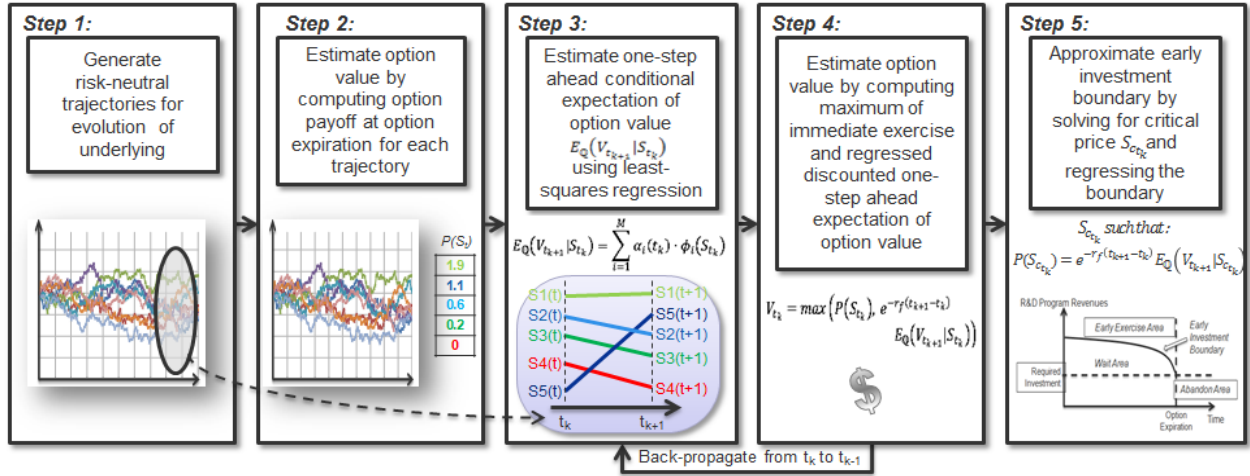


Figure 5: American and Bermudan option valuation with regression and trigger boundary generation

A subtle difference with the works of Carriere is the choice of realized payoffs as dependent variables for the regression instead of using previously computed conditional expectations. These realized payoffs may be resulting from an early-exercise at the next time step t_{k+1} or from an early-exercise several steps down-the trajectory, for instance at t_{k+j} ($j > 1$). According to Longstaff and Schwartz, this precludes “an upward bias in the value of the option”. This means that the conditional expectation at time t_k denoted by $E_{\mathbb{Q}}(V_{t_{k+1}}|S_{t_k})$ is used just once in the algorithm to check whether the value of holding the option is greater than the value of immediate exercise. This yields the following exercise rule and option value highlighted in Eq. 10. Let’s notice the subtle difference with Eq. 9 in the value of the option (the exercise rule remains the same).

$$V_{t_k} = \begin{cases} P(S_{t_k}) & , \text{if } P(S_{t_k}) \geq e^{-r_f(t_{k+1}-t_k)} \sum_{i=1}^M \alpha_i(t_k) \cdot \phi_i(S_{t_k}) \\ e^{-r_f(t_{k+1}-t_k)} \cdot V_{t_{k+1}} & , \text{if } P(S_{t_k}) < e^{-r_f(t_{k+1}-t_k)} \sum_{i=1}^M \alpha_i(t_k) \cdot \phi_i(S_{t_k}) \end{cases} \quad \text{Eq. 10}$$

2.4.2 Generating the trigger boundary

The next objective is to solve for the trigger boundary in order to provide decision-makers with relevant data to substantiate whether investing now or later is optimal. The trigger boundary is made of critical prices which are defined as the time-indexed business prospect values such that keeping the real option open (waiting) has the same value as exercising the option immediately (investing). Using the conditional expectation regressions obtained in the Longstaff-Schwartz algorithm, the critical prices $S_{t_k}^C$ are obtained at each time step t_k by solving Eq. 11.

$$P(S_{t_k}^C) = e^{-r_f(t_{k+1}-t_k)} \sum_{i=1}^M \alpha_i(t_k) \cdot \phi_i(S_{t_k}^C) \quad \text{Eq. 11}$$

2.4.1 Estimating the expected time to trigger and the probability of trigger

Once the early exercise boundary location is known, the expected time to hit the trigger boundary conditional on hitting it, as well as the actual probability of exercising the real option can be computed using (Quasi-) Monte Carlo simulations as highlighted in Eq. 12. In this equation, $E(\tau)$ is the expected time to hit the trigger boundary, $P_{Exercise}$ is the probability of hitting the trigger boundary, τ is the discrete-time equivalent of a stopping

time, T is the maturity of the option, n is the number of trajectories in the simulation, while n^* is the number of trajectories hitting the trigger boundary. The simulations are carried out under the physical probability measure since the expected time to hit and the probability of hitting depend on the real drift of the stochastic process. The expected time to hit the boundary is interesting as it gives an indication of how much time is available before the company is expected to invest: in the case of R&D programs, the expected time to hit the trigger boundary suggests the time left to improve the performance and mature technologies that are projected to be used during the development.

$$E(\tau) = \frac{1}{n^*} \sum_{i=1}^n \tau_i \cdot \mathbf{1}_{\tau_i \leq T} \quad \text{and} \quad P_{Exercise} = \frac{n^*}{n} \quad \text{Eq. 12}$$

$$\text{with: } \tau_i = \min_k (t_k \geq 0 / S_{t_k}^i \geq S_{t_k}^c) \quad \text{and} \quad n^* = \sum_{i=1}^n \mathbf{1}_{\tau_i \leq T}$$

2.5 Summary of the proposed methodology

Having described the different steps of the proposed methodology to value real options with early-exercise privileges, the diagram in Figure 6 summarizes the techniques used and depicts the flow of information between the various steps.

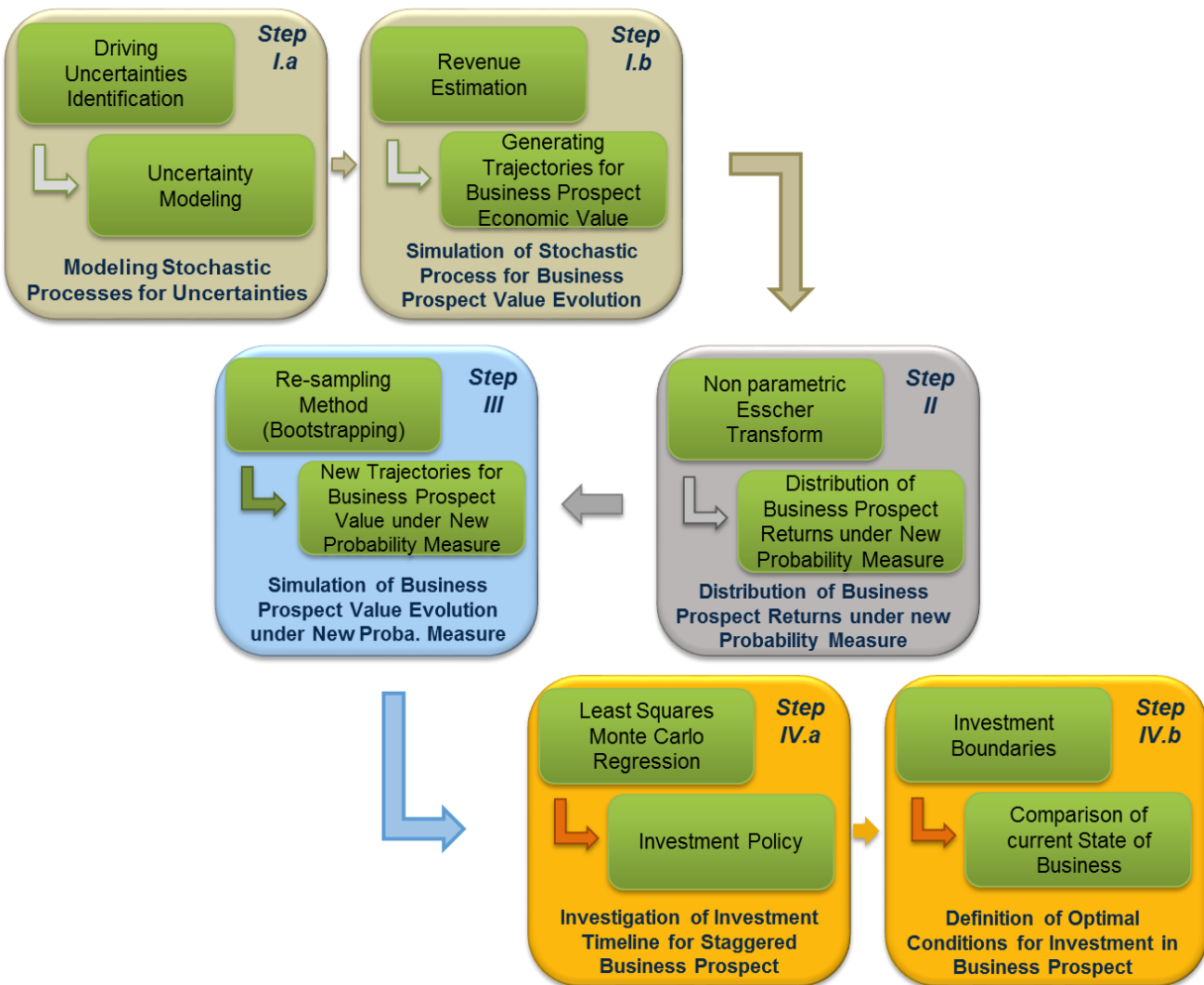


Figure 6: Main steps of the proposed methodology

2.6 Meeting the Georgetown Challenge?

This article started with the *Georgetown Challenge* (Copeland and Antikarov [9]) which is a set of requirements identified by academics and practitioners that real option analyses must meet in order to get wider acceptance. In the previous section, a methodology is constructed step-by-step to analyze long-term staggered corporate investments featuring flexibility. It is therefore appropriate to revisit these key challenges identified earlier and to verify whether the proposed way-forward meets some of these requirements. Table 2 maps the requirements of the *Georgetown Challenge* as well as some specific challenges identified as part of this research, to the assumptions, techniques, and solutions shaping the proposed methodology.

Table 2: Addressing the challenges facing the analysis of long-term corporate investment programs featuring flexibility

		Monte Carlo-based and non-parametric Esscher-transformed real option approach
Georgetown Challenge Requirements (Adapted from Copeland and Antikarov [9])	Intuitively dominate other decision-making methods	<ul style="list-style-type: none"> • Ability to capture the flexibility in decision-making • Recognize the value created by active and astute management
	Capture the reality of the problem	<ul style="list-style-type: none"> • Ability to handle optimum timing issues related to decision-making using American-type options • Ability to handle staggered investment programs with decision gates using compound options
	Use mathematics that everyone can understand	<ul style="list-style-type: none"> • Esscher transform ensures that risk-neutralization is performed in a transparent and tractable way • Non-parametric Esscher transform removes the requirement to calibrate complex models
	Rule out the possibility of mispricing by eliminating arbitrage	<ul style="list-style-type: none"> • Esscher transform provides the price that would be enforced by arbitrageurs in a complete market • Esscher transform provides the price corresponding to the preference of economic agents with iso-elastic utility functions in the case of incomplete markets
	Be empirically testable	<ul style="list-style-type: none"> • Tough requirements as there are no published transacted price for these investments • Only heuristic argumentation can substantiate whether the method provides acceptable solutions
	Appropriately incorporate risk	<ul style="list-style-type: none"> • Handling of technical and market risks separately, with technical risk analyzed with decision trees • Possibly difficult to estimate volatilities of some particular risks if no prior history exists
	Use as much market information as possible	<ul style="list-style-type: none"> • Ability to use market information whenever possible to model the dynamics of the uncertainties driving the development program value
Additional requirements	Ability to capture a complex reality with intertwined uncertainties	<ul style="list-style-type: none"> • Monte Carlo simulations allow the use of many different stochastic behaviors for uncertainties • Monte Carlo simulations allow the modeling of correlations between some sources of uncertainties
	Ability to visualize uncertainties and the decision process	<ul style="list-style-type: none"> • Visualization of the evolution of uncertainties affecting the decision process • Visualization of the evolution of the development program value over time
	Ability to handle corporate investments featuring exotic options	<ul style="list-style-type: none"> • Recent Monte Carlo methods allow analyses of programs with potentially moving decision tollgates and therefore the search for optimum investment timeframes
	Ability to converge to a solution in a timely manner	<ul style="list-style-type: none"> • Use of bootstrapping methods allow a reduction in computation time to generate trajectories of program values used for Monte Carlo simulations

3 Lessons Learnt and Implementation

Preliminary experimentations indicate that the proposed methodology works very well, especially for the valuation of real options. However, the generation of the trigger boundaries using simulation and regressions yields noisy results. Indeed, the nature of Monte Carlo simulations as well as numerical errors introduced by conditional expectation regressions lead to trigger boundaries with jaggies and undesirable local non-monotonicity. This is to be expected and the inaccuracies of trigger boundaries obtained in this manner have been documented in the literature which usually suggests the use of finite-difference methods to obtain reliable and accurate boundaries. However, because the proposed real option framework enables the study of a wide variety of potentially correlated and multi-dimensional stochastic processes, simulation remains an appealing option. As a result, further research is carried out to improve the ability of the least-squares Monte Carlo algorithm to provide better trigger boundaries.

3.1 Refinements to the Longstaff-Schwartz least-squares Monte Carlo algorithm

3.1.1 Control variates sampled at exercise of the real option

The first refinement to the regression-based algorithm consists in using control variates sampled at exercise of the real option. Control variates enable a reduction in the variance of estimates obtained through Monte Carlo simulations by exploiting errors in estimates of known quantities. For instance, it is usual to have the price of a European option as control variate during the pricing of an American option. In this case, the European option price is computed using the same set of trajectories as those used for the pricing of the American option and the European option price estimate $V_{t_0}^{EMC}$ is compared to its known closed-form solution $V_{t_0}^E$ to compute its error. This error is used next to correct the estimate of the American option price $V_{t_0}^{A,MC}$ as shown in Eq. 13.

$$V_{t_0}^A = V_{t_0}^{A,MC} + \theta \cdot (V_{t_0}^{EMC} - V_{t_0}^E), \quad \text{with } \theta = \frac{-Cov(V_{t_0}^{A,MC}, V_{t_0}^{EMC})}{Var(V_{t_0}^{EMC})} \quad \text{Eq. 13}$$

However, control variates sampled at maturity are not efficient for the pricing of options featuring early-exercise possibilities because the correlation between the control variates (sampled at maturity) and the payoffs (sampled at the stopping time) is not large. To improve this correlation, Rasmussen [28] suggests a different sampling scheme for the control variates: instead of sampling the control variates at maturity, the control variates are sampled for each and every simulation path individually at the time of exercise of the American option. This process is highlighted in Figure 7.

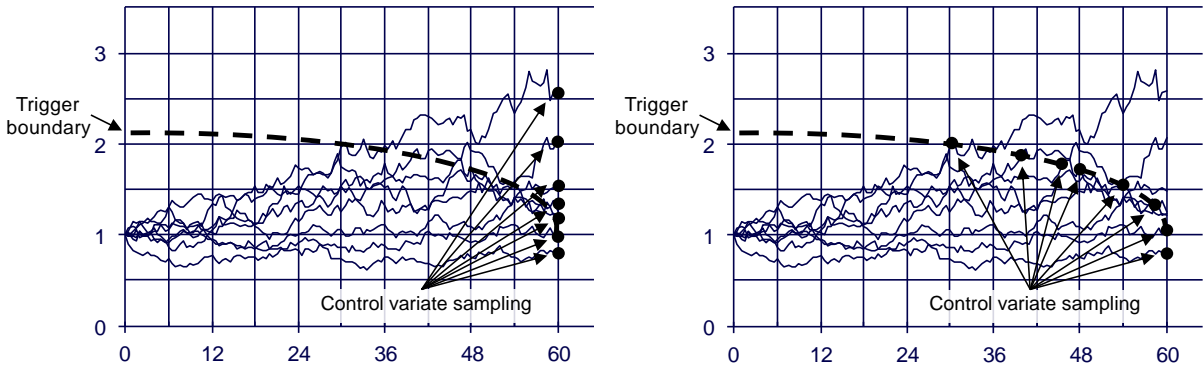


Figure 7: Sampling control variates at maturity (left graph) is less correlated with option payoffs than sampling control variates at exercise (right graph)

Since the aim of the proposed real option methodology is to stay as generic as possible and because the stochastic process representing the evolution of the business prospect value is unknown, using the European option price as control variate is not possible as this quantity is unknown. Instead, we suggest using the discounted business prospect value, which is a martingale by construction, as control variate. The optional stopping theorem ensures that the expected value of the discounted business prospect value at a stopping time is its (known) initial value.

Furthermore, Rasmussen argues [29] that the continuation value regressions may be improved in order to enhance the generation of the trigger boundary. Indeed, if there is a time t_k variable for which the time t_{k-1} conditional expectation is known, then the time t_k variable can be projected onto the same set of basis-functions as those used for the projection of the discounted continuation value and then compared to the t_{k-1} conditional expectation. The error between the projection and the conditional expectation is then used to improve the regression of the discounted continuation value. Again, we suggest using the discounted business prospect value since it is a martingale and therefore its t_{k-1} conditional expectation is always known.

3.1.2 Natural boundary as a lower / upper bound for the estimation of critical prices

Another refinement concerns the size of the domain used during the regression of the one-step-ahead conditional expectation which yields the continuation value. Longstaff and Schwartz (2001) [27] suggest using only in-the-money paths to perform the regression. Still, restricting the regression domain even more might further improve the quality of the conditional expectation regressions: in fact, an even smaller domain of regression may be obtained by using only trajectories deeper in-the-money than the *natural boundary* [28]. Unlike the trigger boundary that is defined as the locus of points for which the holding value exactly matches the immediate exercise value, the natural boundary is defined as the locus of points for which the value of holding the option until maturity exactly matches the immediate exercise value. The difference between the two boundaries is that the trigger boundary is constructed using the holding value with possibility of exercise at any time until maturity (an American real option), while the natural boundary is constructed using the holding value with no possibility of intermediate exercise before maturity (a European real option). Since European options have always less or equal values than American options, the natural boundary yields a locus of points less in-the-money than the corresponding trigger boundary. Besides, the valuation of European options does not require any regression making it straightforward. Therefore, the natural boundary provides a lower bound for the critical prices of an American call option, while it provides an upper bound for the critical prices of an American put option. The reduction of the regression domain is illustrated in Figure 8.

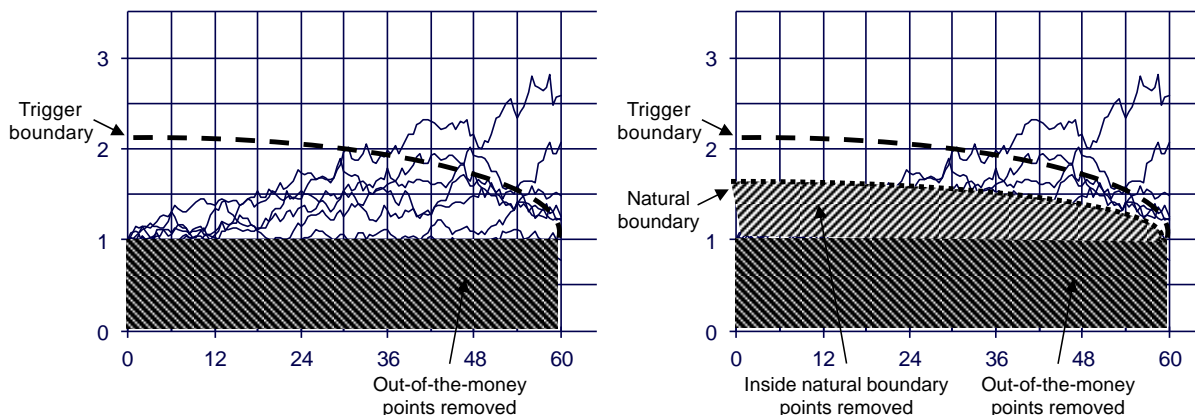


Figure 8: Removing points inside the natural boundary (right graph) scopes down the conditional expectation regression domain and improves the estimation of critical prices for American and Bermudan real options (call option depicted)

The natural boundary can be efficiently computed via simulation, starting right before maturity and marching back in time using just one set of trajectories (in fact a single set of returns from a complete simulation). At each time step t_k starting from the next to last one, bisection is used to search for the value of the business prospect S_{t_k} such that the European option price $V_{t_k}^{EMC}$ is equal to the option immediate payoff P as shown in Eq. 14. At each time step, multiple European option prices must therefore be computed during the search procedure (same option but different spot prices). For each t_k option, the computation is carried out with the same set of returns but with a different simulation starting point. For instance, right before expiration, the European options have a one-step maturity and therefore only returns associated with the first time step of the trajectories are used. For the preceding step, the European options have a two-step maturity and therefore only returns associated with the first two time steps of the trajectories are used. Depending on the accuracy sought for the natural boundary, the procedure is repeated either at every time step or every couple of time steps while marching back in time.

$$V_{t_k}^{EMC}(S_{t_k}) = P(S_{t_k}) \tag{Eq. 14}$$

3.1.3 Multi-start Monte Carlo simulations

The generation of the trigger boundary using Monte Carlo simulations is a notoriously difficult task. The proposed multi-start Monte Carlo improvement stems from the observation that the quality of the least-squares regressions improves as more points and therefore more trajectories lie “in-the-money”. Indeed, with more trajectories “in-the-money”, the regression of the conditional expectation becomes more accurate as more trajectories are likely to cross the trigger boundary thus enhancing the estimation of the critical price. In fact, even when the trigger boundary is reasonably well approximated as a whole, the approximation deteriorates close to the starting time of the simulation. This is a problem of interpolation and extrapolation when searching for the critical price using the conditional expectation regressions. Close to the beginning of the simulation, the effects of diffusion are limited and the business prospect values generated and used for the regression of the conditional expectation are not dispersed enough to encompass or at least to be close to the critical price. Rasmussen [30] suggests starting the simulation prior to the current time (i.e. back in time) in order to let the diffusion artificially disperse the data points and therefore “*to provide sufficient in-the-money observations to estimate the exercise boundary*”.

Even though this is a step in the right direction, this solution does not go far enough and we suggest several improvements. First, the objective should not be to provide a sufficient number of in-the-money observations but rather to provide a sufficient number of observations close to the unknown early-exercise boundary so as to avoid extrapolations during the critical price search since extrapolations are notoriously bad for polynomial regressions (Runge’s phenomenon). Next, this approach is not very efficient computationally-wise as a longer clock-time must be simulated to accommodate the back-in-time starting point. In the generic environment proposed in this paper, this is computationally costly due to the need for resampling. Finally, this approach does not guarantee that the dispersion is sufficient to provide observations close to the critical price. In fact, for at-the-money call options with low risk-free rates and large volatilities, the drift of a geometric Brownian motion under the equivalent martingale measure is usually negative and the proposed approach tends to drive trajectories away from the initial critical prices of the trigger boundary.

Instead, we suggest a multi-start Monte Carlo simulation. This is based on the fact that the position of the trigger boundary is not affected by the initial business prospect value and that using different starting points for the simulations should yield the same boundary. In the multi-start Monte Carlo, we suggest using m different starting points, each having n/m simulations attached, instead of having n simulations starting from a single point in the past. As such, the technique illustrated in Figure 9 does not increase the computational burden. The starting points are chosen so as to maximize the likelihood of “encompassing” the early-exercise boundary while minimizing the

likelihood of sampling the domain where early-exercise is not optimal. This leads to the question of selecting appropriate starting points: the strike price and a multiple of the strike can almost always be used to select two extreme starting points. The initial point of the natural boundary derived previously provides another excellent lowest (largest) starting point for call (put) options. Finally, the domain in between these extreme starting points is evenly distributed to get evenly-spaced simulation starting points.

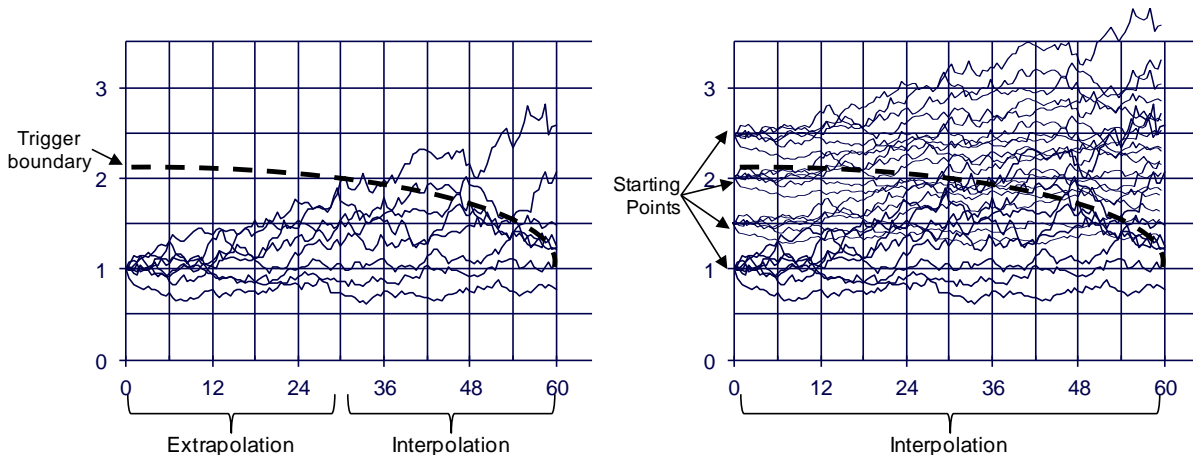


Figure 9: Multi-start simulations enable more interpolations and fewer extrapolations during the critical price search using the one-step-ahead conditional expectation regressions

3.1.4 Quasi-Monte Carlo simulations using low-discrepancy Sobol sequence

Despite the implementation of the previous refinements, there is still some variability in the shape and position of the trigger boundary when repeating identical Monte Carlo experiments. The variability is induced by changes in the seeds used by pseudo-random number generators. The modifications of the trigger boundary shape and position observed during repeated experiments can be attributed to the varying quality of the sequences of pseudo-random numbers used. Consequently, one refinement of the methodology concerns the use of low-discrepancy sequences instead of pseudo-random numbers to generate trajectories of the primary uncertainties under the physical probability measure. Indeed, Jackel [31] argues that low-discrepancy sequences provide superior performance when trying to generate uniformly distributed numbers for the purpose of inverse transform sampling.

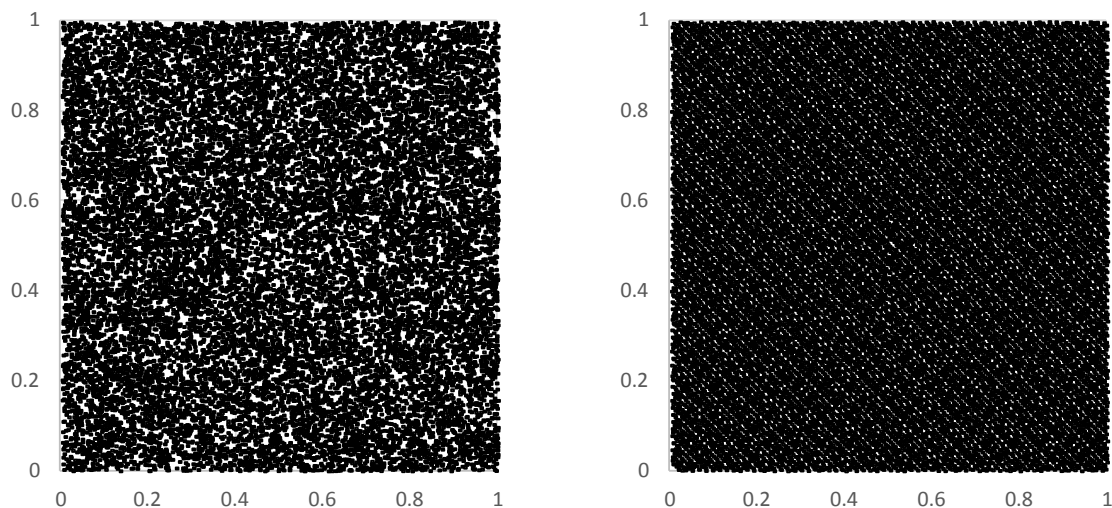


Figure 10: 20,000 uniformly distributed sequences of numbers across two dimensions. Left graph represents pseudo-random numbers from a Mersenne Twister while right graph represents Sobol sequence

This is illustrated in Figure 10 which compares a two-dimensional set of uniformly distributed numbers using the Mersenne Twister implemented within the MS Excel environment and a two-dimensional Sobol sequence: pseudo-random numbers exhibit gaps and clustering while Sobol sequences are evenly distributed. Several low discrepancy sequences may be used for the purpose of Quasi-Monte Carlo simulations like the Van-der-Corput sequence, the Halton sequence, the Niederreiter sequences, and the Sobol sequences [32]. However, many of these sequences are not well suited for high-dimensional applications such as path-dependent options: indeed, each time step represents one dimension and therefore path-dependent options may have several hundred dimensions. Nevertheless, Sobol et al. [33] argue that properly initialized Sobol sequences may be used in high dimension applications. As a result, these sequences are used for this research. Finally, Jackel [31] indicates that the convergence of Quasi-Monte Carlo simulations is not one over the square root of the number of samples (as in traditional Monte Carlo simulations) but rather closer to one over the number of samples which leads to a substantial gain in computational efficiency.

3.1.5 Other refinements

Several other refinements are implemented in order to improve the accuracy of the proposed methodology. Because they have less impact on the generation of the early-exercise boundary and the estimation of the final option price, these improvements are only briefly mentioned:

- *Pooling of Esscher-transformed return samples*

In order to increase the size of the sample of weighted returns from which the bootstrap procedure performs the resampling and in order to decrease the likelihood of drawing repetitively the same highly weighted returns, the return samples from several time cross-sections are pooled together. This enables to bootstrap with a “down-sampling factor” i.e. resampling n observations from a sample of size $k \cdot n$ with k an integer strictly greater than one. This helps mitigate the repetitive sampling of observations with relatively large weights. In addition, in case rare events such as jumps are present, the pooling of several time cross-sections increases the likelihood of capturing these rare events, at least in the original sample.

- *Multi-pass analysis*

Several successive analyses are performed in order to remove the upward bias in the Longstaff and Schwartz algorithm [27]. First, a single set of Quasi-Monte Carlo simulations is used to estimate the natural boundary. This set of returns is recycled for the multi-start simulations enabling the generation of the trigger boundary. Finally, a new set of Quasi-Monte Carlo simulations is used to actually value the real option once the position of the trigger boundary is known.

- *Restricted early-exercise of the option*

Following Rasmussen [29], the early-exercise of the option is performed if and only if the value from immediate exercise is greater than both the value from holding the option one extra time step and the value from holding until maturity (i.e. business prospect value is above natural boundary). This is a safeguard to avoid spurious early-exercise induced by questionable holding value conditional expectation regressions.

- *Regression of the locus of critical prices*

Because the critical prices obtained with the proposed method are noisy and because the trigger boundary is a smooth monotonous curve when dividends (value leakages in the case of real options) are not discrete, the critical prices are regressed in order to yield a smooth and monotonous trigger boundary. At maturity (where a discontinuity may exist), the trigger boundary is fixed to the strike price (investment cost).

- *Multi-pass regression to remove critical-price outliers*

The quality of the critical price regression is affected by the presence of outliers. To mitigate the impact of outliers on the quality of the trigger boundary, the regression is used to compute semi-Studentized residuals (Studentized residual are computationally intensive to estimate as they require the hat matrix). This enables the detection of outliers and their removal prior to performing a second improved regression of the critical prices.

3.2 Implementation choices

In Table 3, the parameters retained for the application and verification of the proposed methodology using canonical examples are summarized. The methodology is implemented in Visual Basic for Application within the MS Excel environment to demonstrate the suitability of the method for use by a wide spectrum of practitioners using development environments typically available to them⁴.

Table 3: Implementation parameters

Number of paths	80,000 / 50,000	Esscher parameter search algorithm	Bisection
Number of time steps	90 / 180	Esscher parameter convergence criteria	Change less than 1.0E-11
Resampling pool size	4	Least-squares regression basis	1 ; $Payoff$; $e^{-Payoff}$
Multi-start simulation starting point number	50	Critical price search algorithm	Newton-Raphson Bisection if N.R. fails
Low discrepancy sequence	Sobol sequence	Trigger boundary regression basis	1 ; $e^{-\tau^{0.33}}$; $\sqrt{\tau}$ τ : time to maturity
Sequence initialization	Discard first 4096 points Randomize	Trigger boundary outlier removal criteria	Semi-Std. Residual >1.96

4 Verification and Validation

The purpose of the verification is to check whether the implementation of the real option evaluation methodology yields correct option prices and accurate trigger boundaries. The similarity between real options and financial options enables the use of financial options to perform the canonical tests required for the verification of the proposed method. Indeed, the real option pricing methodology evaluates both types indifferently but the necessity of “a context” to price real options, the availability of mathematical models to price financial options, and finally, the prolific literature dealing with the pricing of financial options makes the verification of the later more straightforward.

4.1 Verification process

The implementation of the proposed real option analysis is articulated around four successive steps including the Monte Carlo simulation under the physical probability measure, the change of probability measure by

⁴ Ubiquity of MS Excel and VBA within companies is the prime driver for this choice. Execution time is about sixty seconds for the combined pricing of a European option, an American option, the generation of the natural boundary, and the generation of the trigger boundary on a laptop computer featuring an Intel Core i5-3317U processor at 1.7GHz.

means of Esscher transform, the trajectory resampling using bootstrapping under the new measure, and the least-squares Monte Carlo technique to generate the trigger boundary and value the option. It is easier to start the verification process by checking first that the implementation of each individual step performs adequately in a variety of scenarios before moving on to the verification of the entire implementation. In this regards, the verification process follows the “bottom-up” approach of the definition-decomposition and verification-validation V-model diagram. The V-model diagram of Forsberg and Mooz [34] is a graphical representation used in systems engineering which depicts the activities related to the development lifecycle of complex systems. Several variants of the V-diagram have been developed over the years [35] including the one highlighted in Figure 11 which describes adequately a system development process. The model starts with user needs on the upper left and ends with a user validated system on the upper right. In between, the development process is articulated first in a top-down approach starting with a requirement analysis with increasing granularity as development progresses, followed by the design, and leading to the implementation. Next, the development process follows a bottom-up approach as higher levels of assemblies and subsystems are successively verified, leading to a system-level verification, and finally ending with the actual operation of the system.

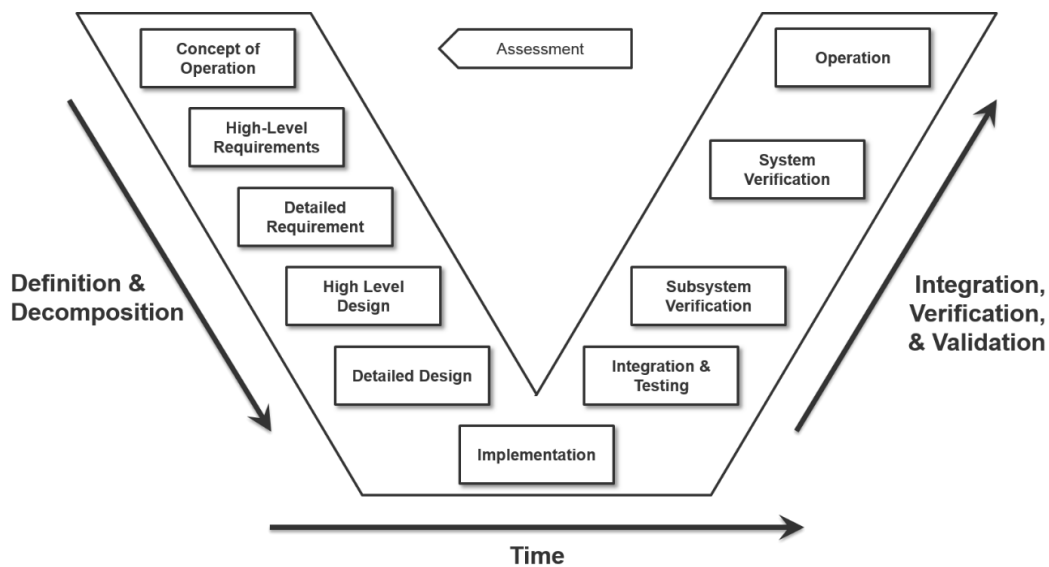


Figure 11: V-Model for systems engineering

Consequently, the different steps of the methodology are verified independently and a verification capability is thus developed to check their outputs. The verification capability requires different verification techniques: some steps yield a single number (such as the option price or the Esscher parameter value), while some steps yield distribution approximations (such as the distribution under the equivalent martingale measure), and finally some other yield two dimensional curved lines (such as the trigger boundary). The wide spectrum of tests to be performed can be decomposed into four different types: visual and graphical methods to check the shape of distributions, statistical tests to check the properties of distributions, similarity tests to check the shape of curves, and numerical comparisons to check quantitative outputs against published results or well established techniques. The verification process is described in Figure 12 with dashed arrows representing verifications of individual modules (subsystem-level) and solid arrows representing verifications of the complete implementation (system-level).

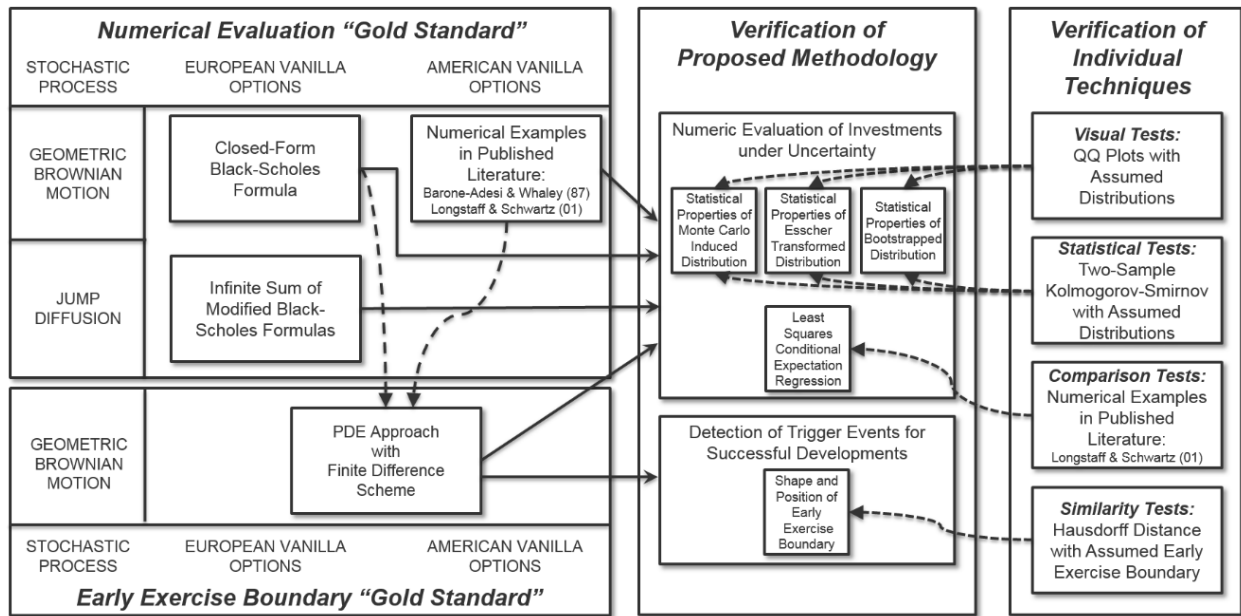


Figure 12: Verification process

4.2 Simulation and non-parametric Esscher transformation

The purpose of the non-parametric Esscher transformation is to transform an arbitrary distribution such that it exhibits risk-neutral properties. The verification starts with a Monte Carlo simulation of the evolutions of primary uncertainties affecting the value of the underlying asset which is then simulated under the equivalent martingale measure using the non-parametric Esscher transform. This yields, at each time step of the simulation, distributions of both underlying asset values and underlying asset returns. The distribution of returns is compared to the known theoretical counterpart. Since one requirement for the proposed real option methodology is the ability to capture a complex reality featuring uncertainties following non-standard stochastic processes, the verification is performed for two completely different processes: a classic geometric Brownian motion (GBM) for which a single equivalent martingale measure exists and the Merton jump-diffusion process (JD) for which the equivalent martingale measure is not unique since the market is incomplete. However, the measure induced by the Esscher transformation leads to one specific combination of jump-diffusion parameters (i.e. new drift, jump arrival rates, and jump amplitudes) which are discussed in Schoutens [36].

Q-Q Plots

One popular technique to compare distributions uses quantile-quantile plot also known as Q-Q plot. A Q-Q plot compares two probability distributions by plotting their quantiles against each other. This non-parametric test enables a quick visualization of whether the location, scale, and skewness of two probability distributions match. In this research, the verification is carried out by plotting the quantiles of the terminal distribution induced by the Monte Carlo simulation and subsequent non-parametric Esscher transformation against the quantiles of the known theoretical terminal distribution. The results for twenty cases of geometric Brownian motions and twenty cases of Merton jump-diffusion processes are provided in ANNEX A.1 and ANNEX A.2 respectively.

For the geometric Brownian motions, all of the plots exhibit locus of quantiles almost perfectly on the bisecting lines. For the Merton jump-diffusion processes, most of the plots are also almost exactly on the bisecting lines. However some of them exhibit some minor deviations, particularly in the extreme ends of the tails (Cases 2, 3, 6, and 18). This may be related to the difficulty of simulating rare events (jumps) in a finite time simulation. If a Q-

Q plot is helpful to qualitatively compare two distributions, it does not however quantify whether the observed deviations are statistically significant.

Kolmogorov-Smirnov tests

It is indeed interesting to quantify these departures from the bisecting lines so as to perform statistical testing and potentially reject the equality of terminal distributions hypothesis. Two popular non-parametric tests are the one-sample and two-sample Kolmogorov-Smirnov tests for the equality between respectively a one-dimensional distribution and a reference distribution or between two one-dimensional probability distributions. The Kolmogorov-Smirnov test computes a “distance” between two distribution functions and establishes the corresponding test statistic. The null hypothesis for these tests is that the samples induced by the simulations followed by non-parametric Esscher transformations are drawn from the known theoretical distributions. This yields test statistics (and p -values) that can be compared to critical values to assess the likelihood of observing such difference between the empirical sample and the reference given the hypothesis that they are sampled from the same distribution.

The results of the Kolmogorov-Smirnov tests for various cases of geometric Brownian motions and Merton jump-diffusion processes are provided respectively in ANNEX B.1 and ANNEX B.2. One-sample Kolmogorov-Smirnov tests are used for geometric Brownian motion cases because the terminal distributions are known, while two-sample Kolmogorov-Smirnov tests are used for Merton jump-diffusion processes since a close-form analytical expression for the terminal distribution is not available and simulation is used to generate reference samples. A five percent level of significance is retained for these tests and the Kolmogorov-Smirnov tests are unable to reject the null hypothesis at this level of significance for both the geometric Brownian motions and the Merton jump-diffusion processes. To account for the variability of results due to randomized Quasi-Monte Carlo simulations, each of the twenty cases is repeated thirty times leading to an experiment consisting of six hundred tests for each process. This yields the distributions of p -values shown in Figure 13 for geometric Brownian motions and in Figure 14 for Merton jump-diffusion processes. The low number of cases with p -values below five percent does not allow the rejection of the null hypothesis.

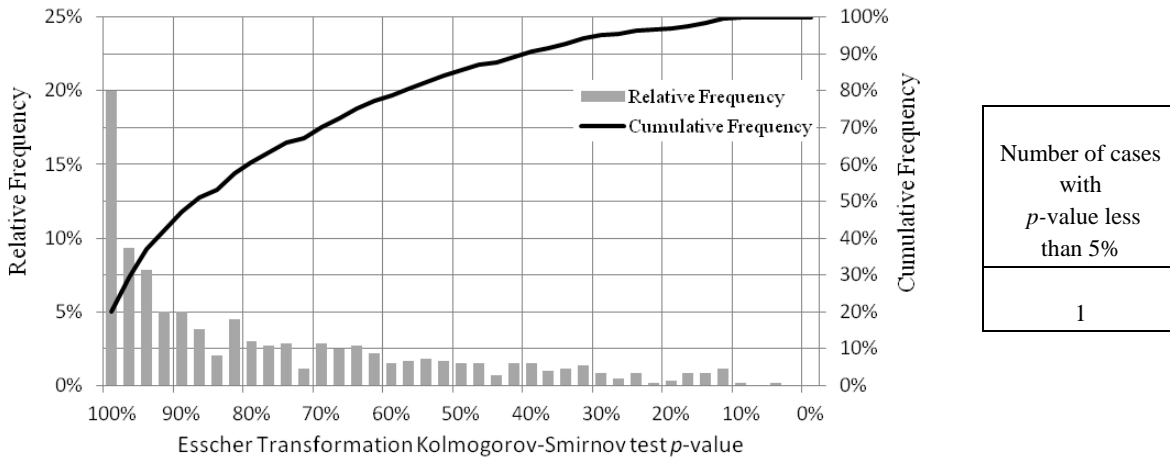


Figure 13: Distribution of p -values for 600 Kolmogorov-Smirnov tests for geometric Brownian motions

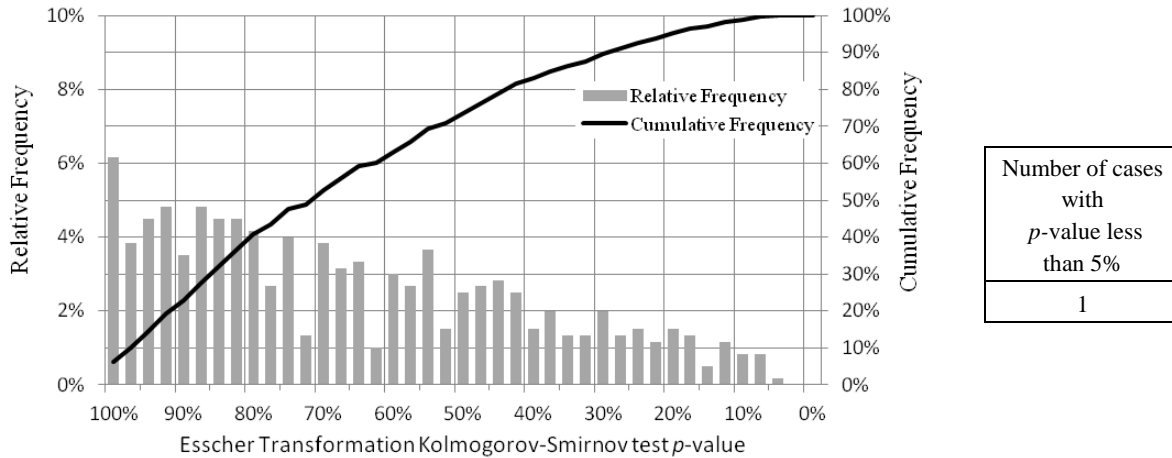


Figure 14: Distribution of p -values for 600 Kolmogorov-Smirnov tests for Merton jump-diffusion processes

Checking the mean with z-test and t-test

Since the change of probability measure often results in a change of drift of the stochastic process, comparing the mean of the terminal distribution of returns induced by Monte Carlo simulations and subsequent non-parametric Esscher transformation to the known theoretical mean is an appealing verification. Like in the previous test, to account for the variability introduced by randomized Quasi-Monte Carlo simulations, each of the twenty cases of geometric Brownian motions and each of the twenty cases of Merton jump-diffusion processes is repeated thirty times to establish a sample average of the terminal distribution mean and the corresponding standard error. The null hypothesis for the tests is that the theoretical mean and the mean of the return distribution induced by Monte Carlo simulations and subsequent non-parametric Esscher transformations are equal. This enables the computation of the z -test statistics (large sample approximation), the Student t -test statistics, as well as the corresponding p -values. The results are provided in ANNEX C.1 for the geometric Brownian motions and in ANNEX C.2 for the Merton jump-diffusion processes.

A five percent level of significance is retained for these tests. Most of the tests exhibit p -values substantially above five percent. Therefore, the z -tests and t -tests fail to reject the null hypothesis at this level of significance for the two stochastic processes.

4.3 Combined simulation, non-parametric Esscher transformation, and bootstrapping

The purpose of the resampling via bootstrapping is to obtain non-weighted trajectories representing the evolution of the underlying business prospect value under the equivalent martingale measure using an initial distribution of weighted returns. The stationary and increment independence properties of the underlying process are used again to sample with replacement from a pool of weighted returns corresponding to the first four time cross-sections of returns obtained from the Quasi-Monte Carlo simulation. Resampling leads to the generation of new trajectories that induce terminal distributions of the business prospect values and their returns. Verification of the combined simulation, non-parametric Esscher transform, and bootstrapping is performed by comparing the properties of the induced distributions with the known theoretical counterparts. The same set of visual and statistical tests are performed.

Q-Q Plots

The results for twenty cases of geometric Brownian motions and twenty cases of Merton jump-diffusion processes are provided respectively in ANNEX D.1 and ANNEX D.2. For the geometric Brownian motions, all of the plots exhibit locus of quantiles almost perfectly on the bisecting lines. For the Merton jump-diffusion processes,

most of the plots are also almost on the bisecting lines. Some of them exhibit nonetheless some minor deviations, particularly in the extreme ends of the tails (Cases 4, 5, 6, 10, and 11).

Kolmogorov-Smirnov tests

The results of Kolmogorov-Smirnov tests for twenty cases of geometric Brownian motions and twenty cases of Merton jump-diffusion processes are provided respectively in ANNEX E.1 and ANNEX E.2. A five percent level of significance is retained. The tests are unable to reject the null hypothesis at this level of significance for both stochastic processes. In order to account for the variability of results due to randomized Quasi-Monte Carlo simulations, each of the twenty cases is repeated thirty times leading to an experiment consisting of six hundred tests for each process. This yields the distributions of p -values shown in Figure 15 for geometric Brownian motions and in Figure 16 for Merton jump-diffusion processes. Again, few outcomes fall below the five percent level of significance which precludes the rejection of the null hypothesis.

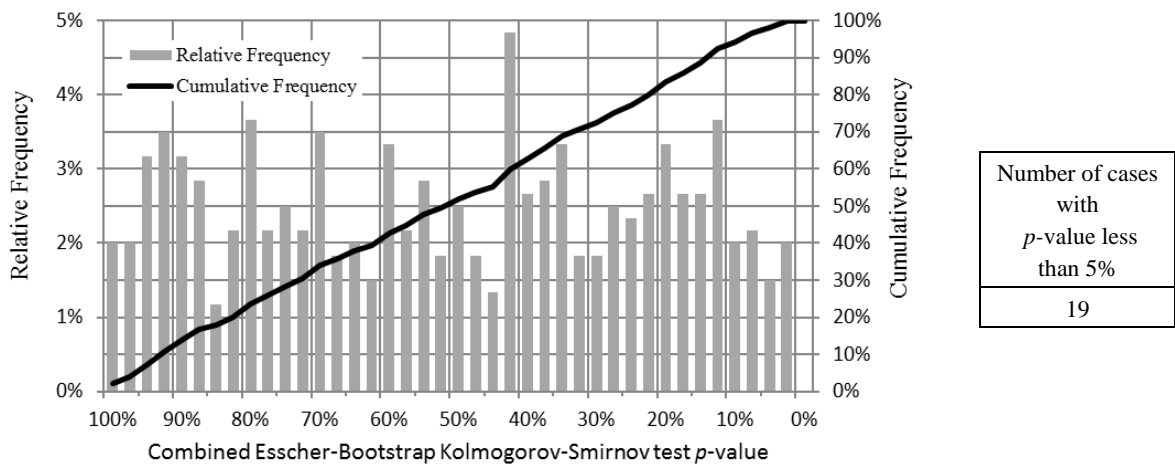


Figure 15: Distribution of p -values for 600 Kolmogorov-Smirnov tests for geometric Brownian motions

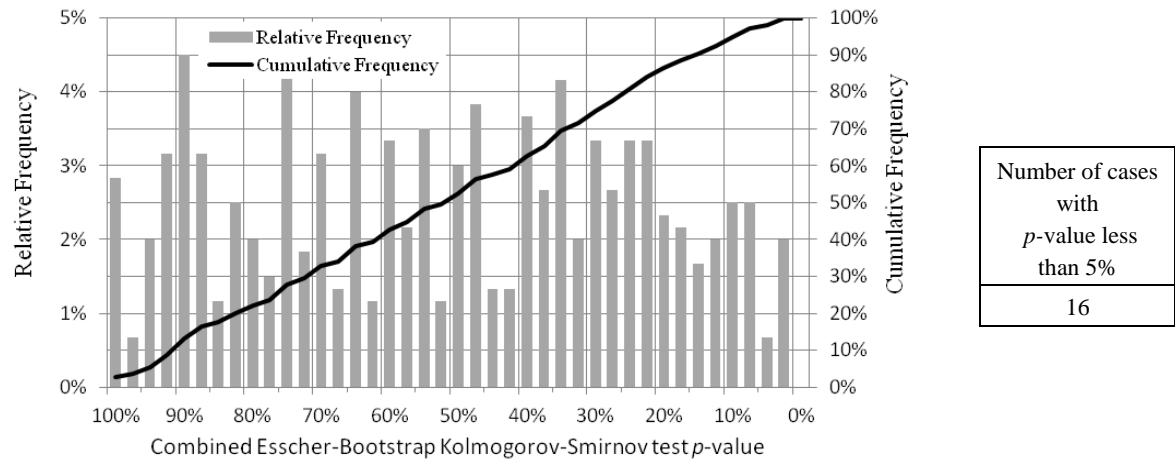


Figure 16: Distribution of p -values for 600 Kolmogorov-Smirnov tests for Merton jump-diffusion processes

Checking the mean with z-test and t-test

The results of z-tests and Student's *t*-tests for twenty cases of geometric Brownian motions and twenty cases of Merton jump-diffusion processes are provided respectively in ANNEX F.1 and ANNEX F.2. A five percent level of significance is retained for the z-tests and *t*-tests. Both the z-tests and *t*-tests are unable to reject the null hypothesis at this level of significance for the two stochastic processes.

4.4 Early-exercise boundary

In order to verify the shape of the early-exercise boundary, a benchmark is first established using an implicit finite-difference scheme. This serves as a reference to test the early-exercise boundary obtained using the proposed methodology. Having a reference early-exercise boundary, an acceptable metric must be used to evaluate how the two boundaries match. The closeness of these two curves is assessed using the concept of Hausdorff distance [37] used in computer graphics to perform digital shape recognition. The Hausdorff distance δ_H between the curves \mathcal{C}_1 and \mathcal{C}_2 is expressed as the maximum of the two directed Hausdorff distances $\delta_{\mathcal{C}_1, \mathcal{C}_2}$ and $\delta_{\mathcal{C}_2, \mathcal{C}_1}$ computed using the Euclidian norm. In turn, the directed Hausdorff distance is the greatest of all the distances from a point in one curve to the closest point in the other curve. The Hausdorff distance therefore measures how far two subsets of a metric space are from each other. For the verification process, the symmetric Hausdorff distance defined in Eq. 15 is used.

$$\delta_H = \max(\delta_{\mathcal{C}_1, \mathcal{C}_2}, \delta_{\mathcal{C}_2, \mathcal{C}_1}) \text{ with } \delta_{\mathcal{C}_1, \mathcal{C}_2} = \max_{x \in \mathcal{C}_1} \left[\min_{y \in \mathcal{C}_2} \|x - y\| \right] \quad \text{Eq. 15}$$

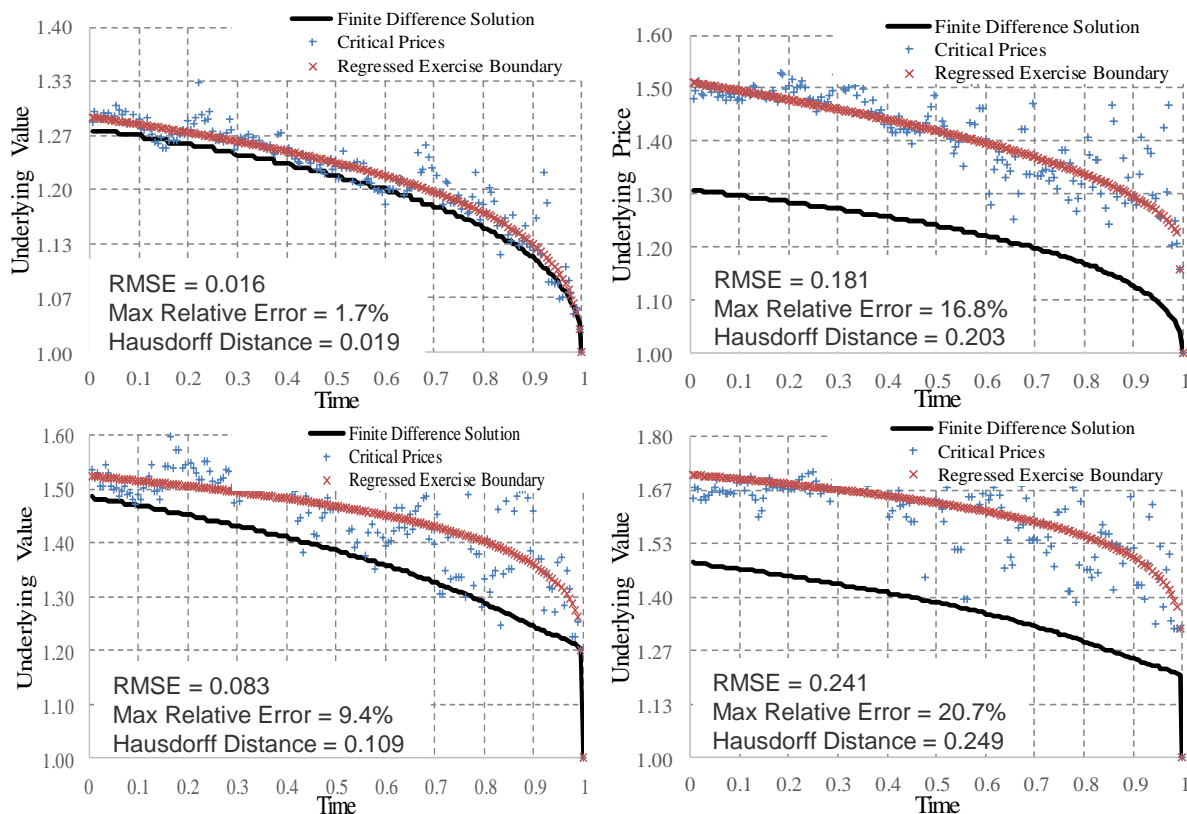


Figure 17: Four cases of early-exercise boundaries; Hausdorff distances to the reference boundaries obtained with finite-difference methods are indicated as well as other error metrics.

The Hausdorff distance is not a relative quantity making numerical results somewhat difficult to interpret and conclusions difficult to establish. However, a unit strike price is used in the different verifications performed making normalization useless. For the sake of clarity, a set of four different trigger boundaries is provided in Figure 17. Hausdorff distances between the trigger boundaries and reference boundaries are provided as well as other error metrics (Root Mean Square Error and maximum relative error). In these graphs, the blue dots represent critical prices, the red lines represent the interpolation of these critical prices, and the black lines represent the reference boundaries. As may be seen, Hausdorff distances above 0.1 correspond to cases where the shapes of the boundaries start to differ significantly from the reference boundaries. Consequently, the threshold of 0.1 is retained to determine a failure in the verification.

The results for twenty different cases of geometric Brownian motions are provided in ANNEX G. All of the Hausdorff distances remain small, with values less than 0.07 in most cases, indicating a close match between the trigger boundaries obtained with the proposed methodology and the reference trigger boundaries obtained via finite-difference methods. Therefore, the verification is considered successful.

4.5 European and American option pricing

The main goal of this research is to provide decision-makers with an estimate of what the business prospect is worth when all real options are accounted for. Therefore, the estimation of real option prices as well as the analysis of its accuracy is crucial to the verification of the proposed methodology. European option prices computed using the proposed methodology are compared to European option prices computed using the analytical expression of Black and Scholes. American option prices are compared to prices obtained using finite-difference schemes for geometric Brownian motions. For jump-diffusion processes, the European option prices are compared to Merton's analytical formula for jump-diffusion processes using the Esscher equivalent martingale measure adjustment. The results are provided in ANNEX H.1 and ANNEX H.2 and show excellent accuracy: the relative error never exceeds 1.5% for geometric Brownian motions and 3.4% for Merton jump-diffusion processes.

The location of trigger boundaries of call options when the business prospect value follows a geometric Brownian motion can be substantially different from when the underlying follows a jump-diffusion process. This is highlighted in Figure 18 which shows the trigger boundaries for two American call options based on processes having the same drift and the same diffusion. One process features jumps and exhibits a deeper-in-the-money trigger boundary than the other. As a result, this impacts the expected time to trigger: starting with a business prospect value of one, the hitting time conditional expectation is just 0.68 year for the pure diffusion process while it reaches 0.84 year for the jump-diffusion process.

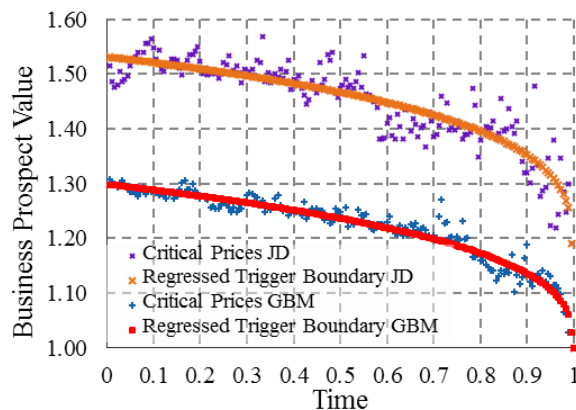


Figure 18: Trigger boundaries for call options ($r_f = 0.02$; $q = 0.05$; $K = 1.00$; $T = 1.00$) with underlying following a geometric Brownian motion ($\mu = 0.20$; $\sigma = 0.20$) and a jump diffusion process ($\mu = 0.20$; $\sigma = 0.20$; $\lambda = 1.00$; $\gamma = -\delta^2/2$; $\delta = 0.20$)

5 Conclusion

In this research, a new methodology for the analysis of investments using a real option approach is proposed. By cross-fertilizing elements from financial engineering, actuarial sciences, and statistics, this research has enabled the development of a traceable and transparent framework for the analysis of staggered corporate

investments featuring timing flexibility. Many of the techniques shaping this methodology are well accepted and already in use in the finance community which may help acceptance by practitioners. The methodology is articulated around four main points: a simulation of the evolution of the value of a business prospect over time under the physical probability measure, a non-parametric Esscher transformation to yield an evolution of the business prospect value under the equivalent martingale measure, a resampling to yield non-weighted business prospect value evolution under this new measure, and finally an option analysis using regressions to both generate trigger boundaries and to value real options featuring timing flexibility.

The proposed methodology contributes to the field of real option analysis by: 1) having the ability to handle a complex reality featuring intertwined uncertainties following non-standard stochastic processes, 2) having the ability to simulate the evolution of the underlying business prospect without requiring the (subjective) specification of a stochastic process, 3) transforming the dynamics of the underlying business prospect value to express them under one equivalent martingale measure without any user input. Several refinements to the acclaimed least-squares Monte Carlo algorithm are also reviewed. Besides, to improve the generation of the trigger boundary, the authors suggest the use of a multi-start simulation with a set of initial values deeper in-the-money than the natural boundary.

The methodology is implemented in a ubiquitous development environment and is verified using a batch of graphical, statistical, and similarity tests applied to several canonical examples. Results for the valuation of options and the generation of trigger boundaries are in agreement with theoretical results, and the execution time is competitive with other real option methods.

Acknowledgements

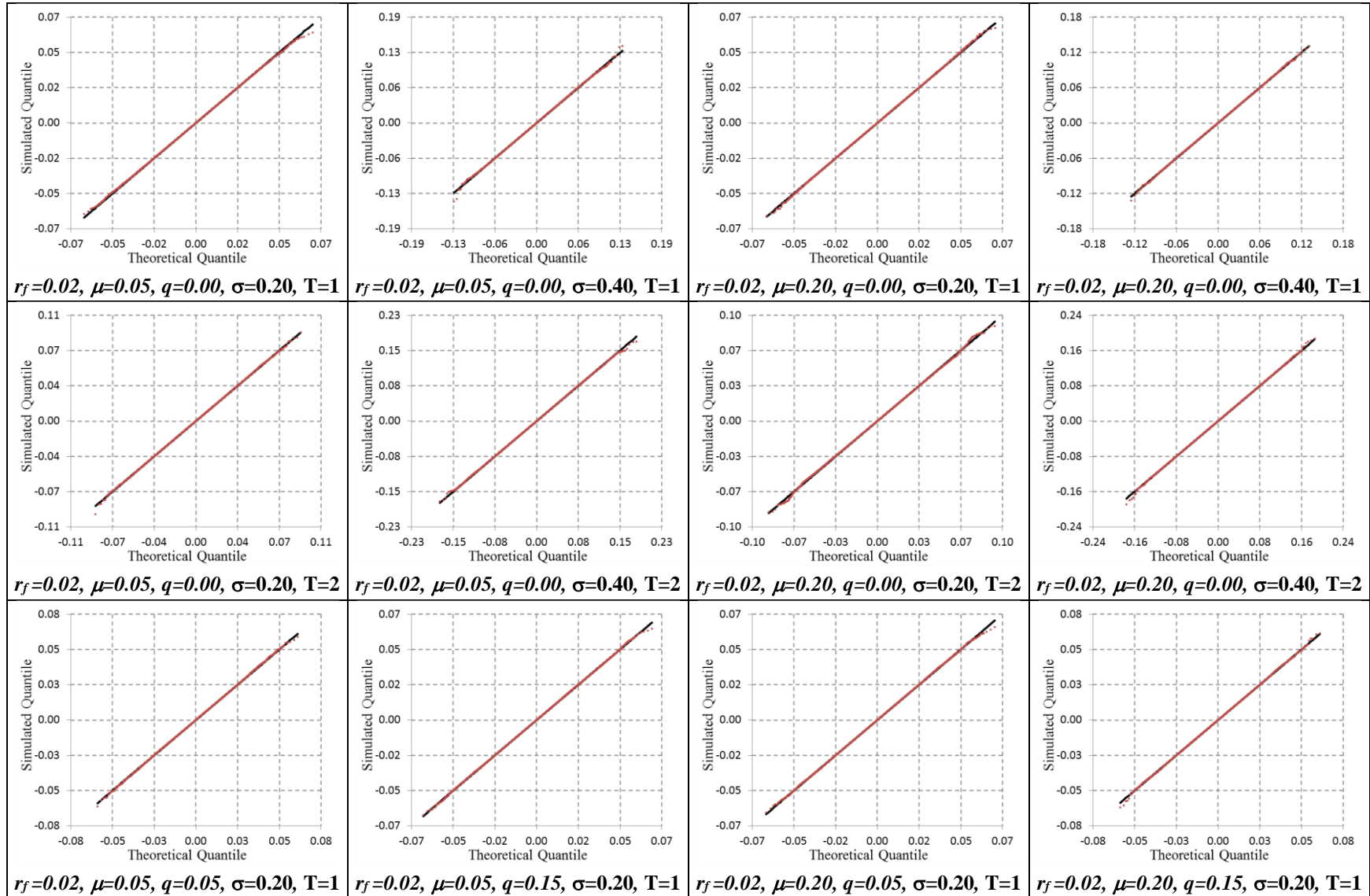
The authors wish to thank Graham Davis for helpful comments and ideas that helped improve the quality of this paper.

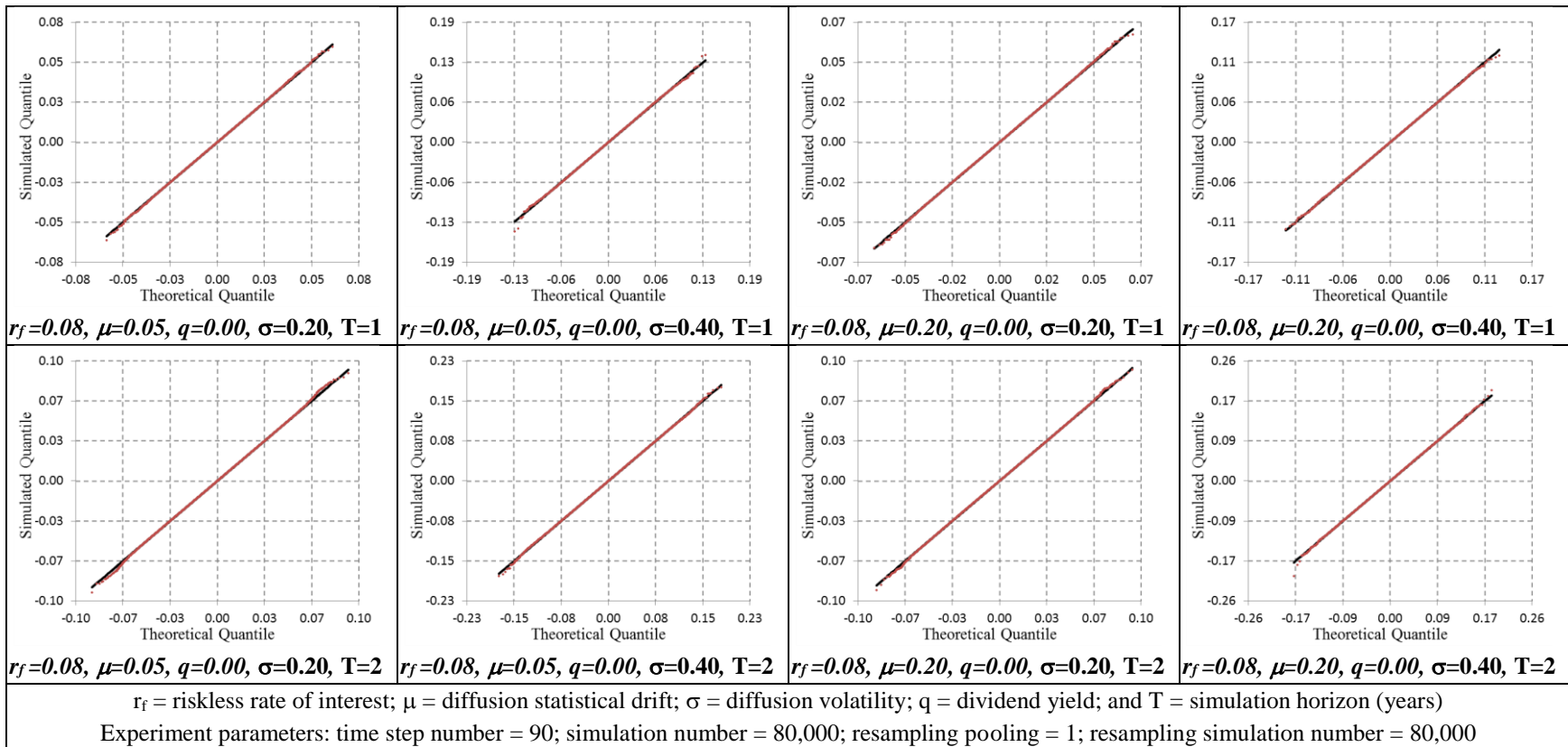
References

- [1] J. Graham and C. Harvey, "The theory and practice of corporate finance: evidence from the field," *Journal of Financial Economics*, vol. 60, pp. 187-243, 2001.
- [2] A. Dixit and R. Pindyck, *Investment under uncertainty*, Princeton University Press, 1994.
- [3] S. C. Myers, "Determinants of corporate borrowing," *Journal of Financial Economics*, vol. 5, no. 2, pp. 147-175, 1977.
- [4] F. Black and M. Scholes, "The pricing of options and corporate liabilities," *Journal of Political Economy*, vol. 81, no. 3, pp. 637-654, May - Jun 1973.
- [5] R. C. Merton, "Theory of rational option pricing," *The Bell Journal of Economics and Management Science*, vol. 4, no. 1, pp. 141-183, 1973.
- [6] M. B. Shackleton, A. E. Tsekrekos and R. Wojakowski, "Strategic entry and market leadership in a two-player real options game," *Journal of Banking and Finance*, vol. 28, pp. 179-201, 2004.
- [7] C. Krychowski, "Apport et limites des options réelles à la décision d'investissement stratégique : une étude appliquée dans le secteur des télécommunications," 2007.
- [8] A. Borison, "Real options analysis: where are the Emperor's clothes?," *Journal of Applied Corporate Finance*, vol. 17, pp. 17-31, 2005.
- [9] T. Copeland and V. Antikarov, "Real options: Meeting the Georgetown challenge," *Journal of Applied Corporate Finance*, vol. 17, pp. 32-51, 2005.
- [10] B. Efron, "Bootstrap methods: another look at the jackknife," *The Annals of Statistics*, vol. 7, pp. 1-26, 1979.
- [11] H. Gerber and E. Shiu, "Option pricing by Esscher transforms," *Transactions of Society of Actuaries*, vol. 46, pp. 99-141, 1994.

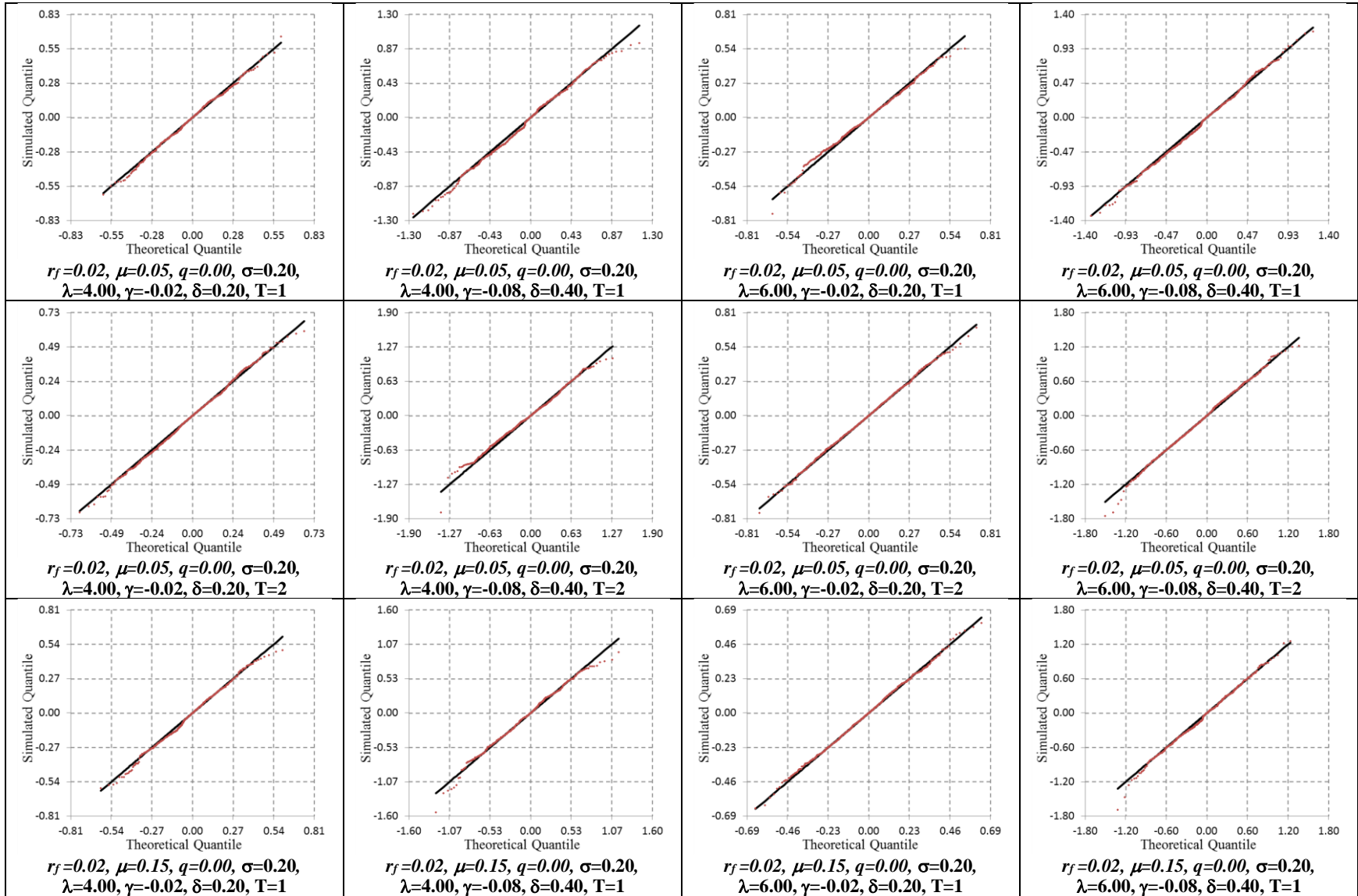
- [12] F. Esscher, "On the probability function in the collective theory of risk," *Scandinavian Actuarial Journal*, vol. 3, pp. 175-195, 1932.
- [13] P. M. Kahn, "An introduction to collective risk theory and its application to stop-loss reinsurance," *Transactions of Society of Actuaries*, vol. 14, pp. 400-449, 1962.
- [14] T. Copeland, T. Koller and J. Murrin, *Valuation. Measuring and managing the value of companies*, Third Edition ed., McKinsey, 2000.
- [15] Y. Miyahara, "A note on Esscher transformed martingale measures for geometric Levy processes," 2004.
- [16] H. Follmer and M. Schweizer, *Encyclopedia of quantitative finance*, Wiley, 2010, pp. 1200-1204.
- [17] M. Frittelli, "Minimal entropy criterion for pricing in one period incomplete markets," 1995.
- [18] H. Gerber and E. Shiu, "Martingale approach to pricing perpetual american options," *Astin Bulletin*, vol. 24, pp. 195-220, November 1994.
- [19] D. Cass and J. Stiglitz, "The structure of investor preferences and asset returns, and separability in portfolio allocation: a contribution to the pure theory of mutual funds," *Journal of Economic Theory*, vol. 2, pp. 122-160, 1970.
- [20] J. Stiglitz, "Theory of valuation: frontiers of modern financial theory," S. Bhattacharya and G. Constantinides, Eds., Rowman & Littlefield Publishers, 1988, pp. 342-356.
- [21] M. Pereira, C. Epprecht and A. Veiga, "Option pricing via nonparametric Esscher transform," Marseille, France, 2011.
- [22] J. M. Harrison and D. M. Kreps, "Martingales and arbitrage in multiperiod securities markets," *Journal of Economic Theory*, vol. 20, pp. 281-408, 1979.
- [23] J. Hull, *Options, futures and other derivatives securities*, 2nd in 1993, 6th ed., Prentice Hall, 2006.
- [24] J. A. Tilley, "Valuing American options in a path simulation model," *Transactions of the Society of Actuaries*, vol. 45, pp. 83-104, 1993.
- [25] J. Carriere, "Valuation of the early-exercise price for options using simulations and non-parametric regression," *Insurance: Mathematics and Economics*, vol. 19, pp. 19-30, 1996.
- [26] L. Stentoft, *Value function approximation or stopping time approximation: a comparison of two recent numerical methods for American option pricing using simulation and regression*, 2008.
- [27] F. Longstaff and E. Schwartz, "Valuing American options by simulation: a simple least-square appr," *The Review of Financial Studies*, vol. 14, pp. 113-147, 2001.
- [28] N. S. Rasmussen, *Efficient control variates for Monte-Carlo valuation of American options*, 2002.
- [29] N. S. Rasmussen, *Improving the Least-Squares Monte-Carlo Approach*, 2002.
- [30] N. S. Rasmussen, "Control variates for Monte Carlo valuation of American options," *Journal of Computational Finance*, vol. 9, no. 1, 09 2005.
- [31] P. Jackel, *Monte Carlo methods in finance*, Wiley Finance, 2002.
- [32] I. Sobol, "On the distribution of points in a cube and the approximate evaluation of integrals," *USSR Computational Mathematics and Mathematical Physics*, vol. 7, no. 4, pp. 86-112, May 1966.
- [33] I. M. Sobol, D. Asotsky, A. Kreinin and S. Kucherenko, "Construction and comparison of high-dimensional Sobol' generators," *Wilmott magazine*, pp. 64-79, 2011.
- [34] K. Forsberg and H. Mooz, "The relationship of system engineering to the project cycle," Chattanooga, TN, 1991.
- [35] D. O. Defense, *Systems Engineering Fundamentals*, Defense Acquisition University Press, 2001.
- [36] W. Schoutens, *Levy processes in finance: pricing financial derivatives*, Chichester, UK: John Wiley and Sons, 2003.
- [37] H. Alt, C. Knauer and C. Wenk, "Comparison of distance measures for planar curves," *Algorithmica*, vol. 38, pp. 45-58, 2004.

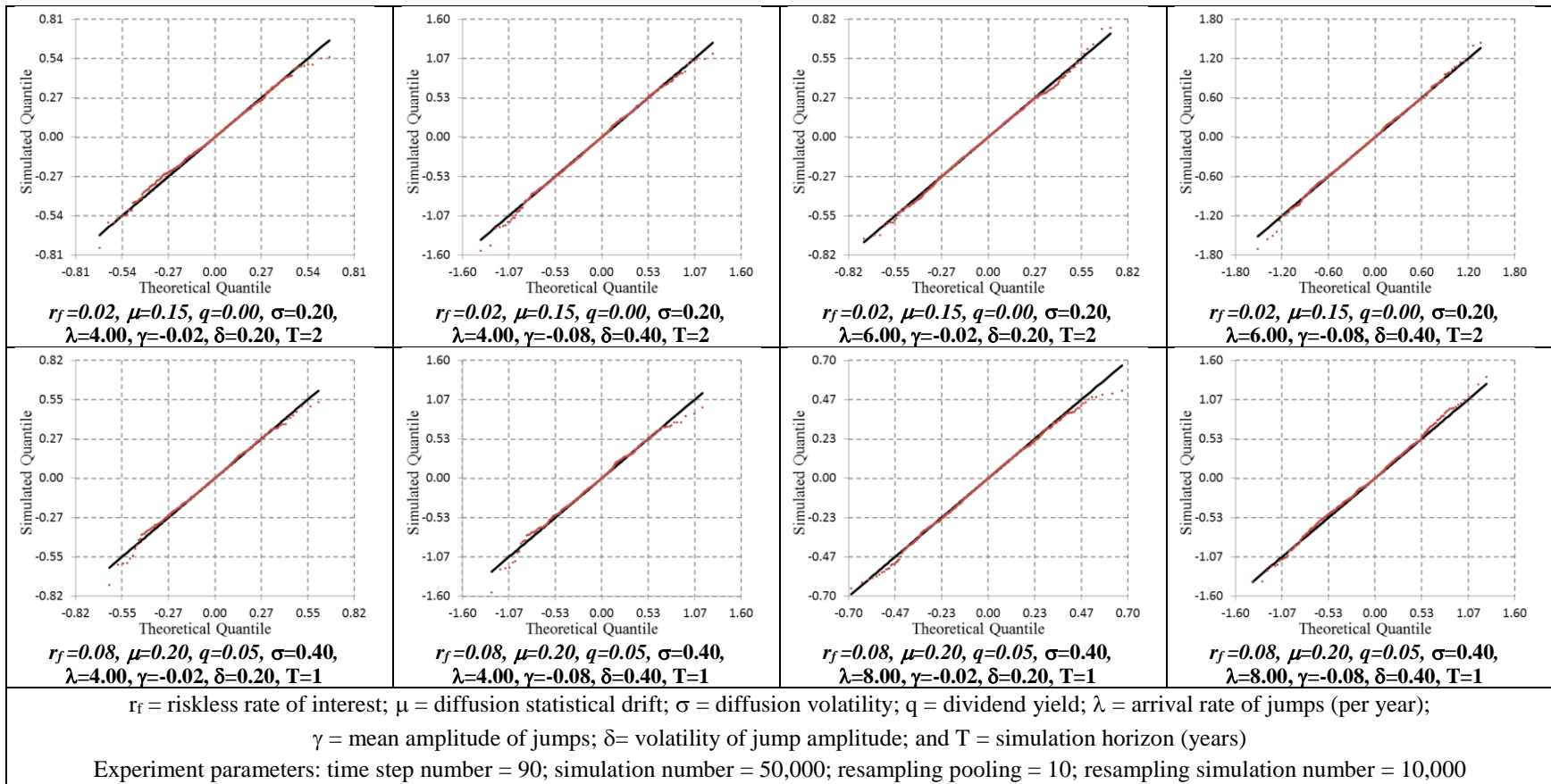
ANNEX A.1: Q-Q plots for distributions induced by non-parametric Esscher transforms of geometric Brownian motions





ANNEX A.2: Q-Q plots for the distributions induced by non-parametric Esscher transforms of jump-diffusion processes





ANNEX B.1: Kolmogorov-Smirnov tests for the distributions induced by non-parametric Esscher transforms of twenty cases of geometric Brownian motions

r_f	μ	q	σ	T	Kolmogorov Smirnov statistic	p -value
2.0%	5%	0%	20%	1.0	0.500	96%
2.0%	20%	0%	20%	1.0	0.392	100%
2.0%	5%	0%	40%	1.0	0.530	94%
2.0%	20%	0%	40%	1.0	0.481	98%
8.0%	5%	0%	20%	1.0	0.937	34%
8.0%	20%	0%	20%	1.0	0.578	89%
8.0%	5%	0%	40%	1.0	0.630	82%
8.0%	20%	0%	40%	1.0	0.877	43%
2.0%	5%	0%	20%	2.0	0.356	100%
2.0%	20%	0%	20%	2.0	0.953	32%
2.0%	5%	0%	40%	2.0	0.586	88%
2.0%	20%	0%	40%	2.0	0.927	36%
8.0%	5%	0%	20%	2.0	0.718	68%
8.0%	20%	0%	20%	2.0	0.580	89%
8.0%	5%	0%	40%	2.0	0.560	91%
8.0%	20%	0%	40%	2.0	0.563	91%
2.0%	5%	5%	20%	1.0	0.597	87%
2.0%	20%	5%	20%	1.0	0.991	28%
2.0%	5%	15%	20%	1.0	0.498	97%
2.0%	20%	15%	20%	1.0	0.503	96%
r_f = riskless rate of interest; μ = diffusion statistical drift; σ = diffusion volatility; q = dividend yield; T = simulation horizon (years) Experiment parameters: time step number = 90; simulation number = 80,000; pooling = 1; resampling simulation number = 80,000						

ANNEX B.2: Kolmogorov-Smirnov tests for the distributions induced by non-parametric Esscher transforms of twenty cases of Merton jump-diffusion processes

r_f	μ	q	σ	λ	δ	T	Kolmogorov Smirnov statistic	p -value
2.0%	5%	0.0%	20%	400%	20%	1.0	0.717	68%
2.0%	5%	0.0%	20%	600%	20%	1.0	0.619	84%
2.0%	5%	0.0%	20%	400%	40%	1.0	0.560	91%
2.0%	5%	0.0%	20%	600%	40%	1.0	0.610	85%
2.0%	15%	0.0%	20%	400%	20%	1.0	0.866	44%
2.0%	15%	0.0%	20%	600%	20%	1.0	0.687	73%
2.0%	15%	0.0%	20%	400%	40%	1.0	0.882	42%
2.0%	15%	0.0%	20%	600%	40%	1.0	0.647	80%
2.0%	5%	0.0%	20%	400%	20%	2.0	0.916	37%
2.0%	5%	0.0%	20%	600%	20%	2.0	0.848	47%
2.0%	5%	0.0%	20%	400%	40%	2.0	0.716	68%
2.0%	5%	0.0%	20%	600%	40%	2.0	0.600	86%
2.0%	15%	0.0%	20%	400%	20%	2.0	0.860	45%
2.0%	15%	0.0%	20%	600%	20%	2.0	0.551	92%
2.0%	15%	0.0%	20%	400%	40%	2.0	1.101	18%
2.0%	15%	0.0%	20%	600%	40%	2.0	0.567	90%
8.0%	20%	5.0%	40%	400%	20%	1.0	1.006	26%
8.0%	20%	5.0%	40%	800%	20%	1.0	0.837	49%
8.0%	20%	5.0%	40%	400%	40%	1.0	0.833	49%
8.0%	20%	5.0%	40%	800%	40%	1.0	0.638	81%
<p>r_f = riskless rate of interest; μ = diffusion statistical drift; σ = diffusion volatility; q = dividend yield; λ = arrival rate of jumps (per year); $\gamma = -\delta^2/2$ = jump amplitude; δ = volatility of jump amplitude; T = simulation horizon (years) Experiment parameters: time step number = 90; simulation number = 50,000; pooling = 10; resampling simulation number = 10,000</p>								

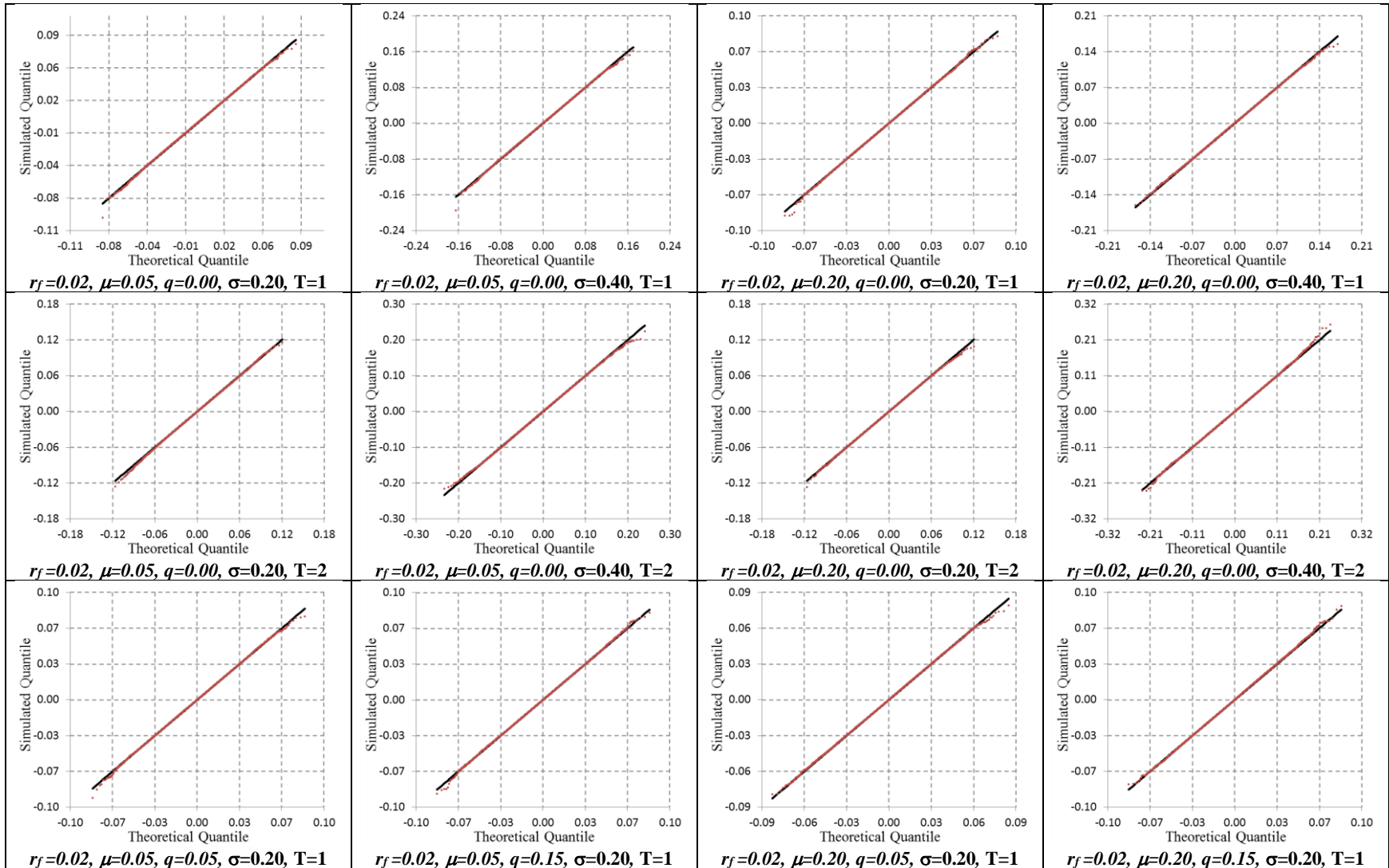
ANNEX C.1: Mean of the distribution induced by non-parametric Esscher transforms of twenty cases of geometric Brownian motions

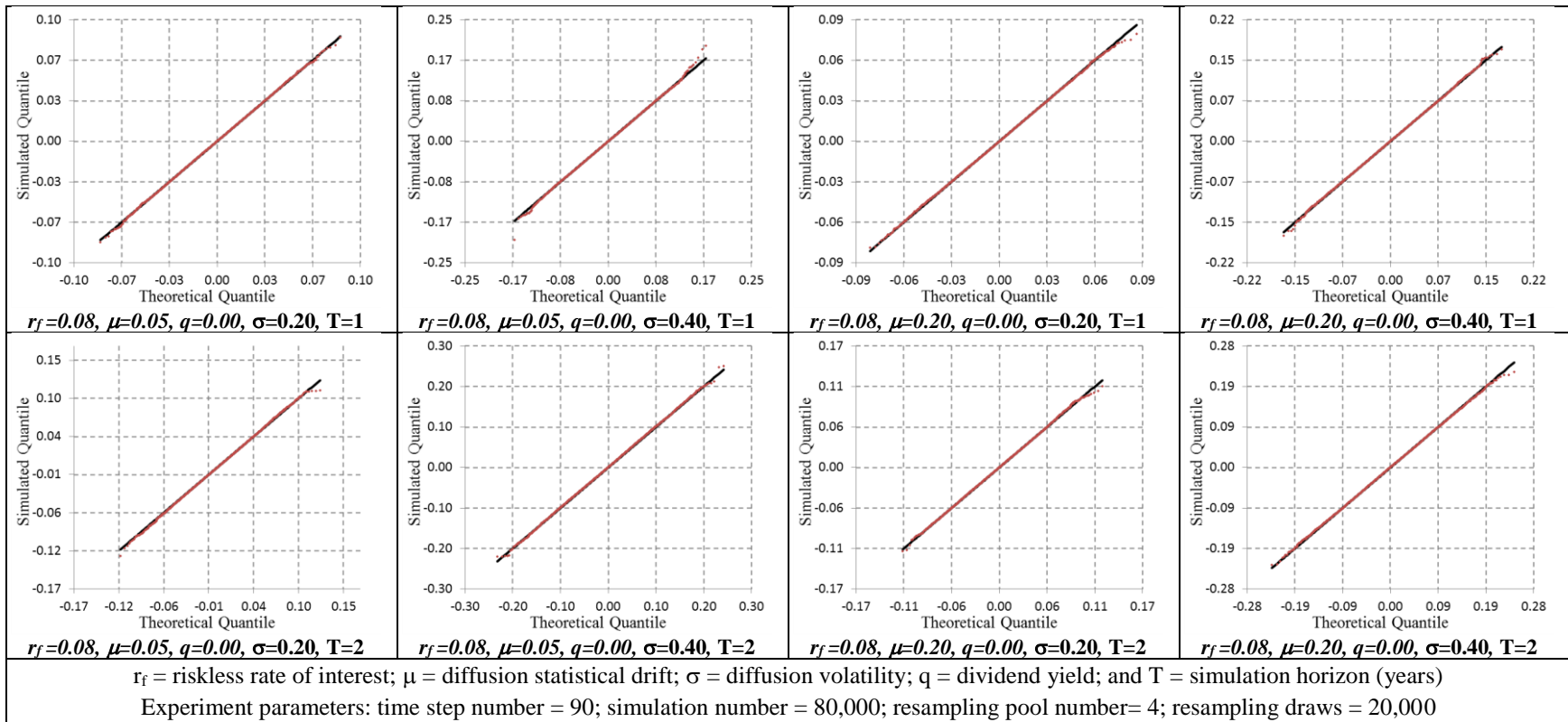
r_f	μ	q	σ	T	Experimental Sample Mean Return	Experimental Sample Standard Error	Theoretical Mean Return	z-test and t-test statistic	z-test p-value	t-test p-value
2%	5%	0%	20%	1	-2.02E-07	1.45E-07	-3.85E-20	1.393	16%	17%
2%	20%	0%	20%	1	1.57E-07	1.10E-07	-3.85E-20	1.436	15%	16%
2%	5%	0%	40%	1	-6.67E-04	5.73E-07	-6.67E-04	0.163	87%	87%
2%	20%	0%	40%	1	-6.67E-04	6.41E-07	-6.67E-04	0.252	80%	80%
8%	5%	0%	20%	1	6.67E-04	1.30E-07	6.67E-04	0.076	94%	94%
8%	20%	0%	20%	1	6.67E-04	1.67E-07	6.67E-04	0.873	38%	39%
8%	5%	0%	40%	1	2.84E-07	5.88E-07	-1.54E-19	0.484	63%	63%
8%	20%	0%	40%	1	-6.27E-07	6.12E-07	-1.54E-19	1.025	31%	31%
2%	5%	0%	20%	2	1.54E-07	1.93E-07	-7.71E-20	0.801	42%	43%
2%	20%	0%	20%	2	1.24E-07	2.58E-07	-7.71E-20	0.482	63%	63%
2%	5%	0%	40%	2	-1.33E-03	1.37E-06	-1.33E-03	0.512	61%	61%
2%	20%	0%	40%	2	-1.33E-03	1.03E-06	-1.33E-03	0.615	54%	54%
8%	5%	0%	20%	2	1.33E-03	3.20E-07	1.33E-03	1.156	25%	26%
8%	20%	0%	20%	2	1.33E-03	2.64E-07	1.33E-03	0.668	50%	51%
8%	5%	0%	40%	2	-1.12E-06	1.05E-06	-3.08E-19	1.063	29%	30%
8%	20%	0%	40%	2	5.36E-07	9.04E-07	-3.08E-19	0.593	55%	56%
2%	5%	5%	20%	1	-5.55E-04	1.43E-07	-5.56E-04	0.659	51%	52%
2%	20%	5%	20%	1	-5.56E-04	1.52E-07	-5.56E-04	1.447	15%	16%
2%	5%	15%	20%	1	-1.67E-03	1.27E-07	-1.67E-03	0.670	50%	51%
2%	20%	15%	20%	1	-1.67E-03	1.50E-07	-1.67E-03	0.563	57%	58%
r_f = riskless rate of interest; μ = diffusion statistical drift; σ = diffusion volatility; q = dividend yield; T = simulation horizon (years) Experiment parameters: time step number = 90; simulation number = 80,000; pooling = 1; resampling simulation number = 80,000										

ANNEX C.2: Mean of the distribution induced by non-parametric Esscher transforms of twenty cases of Merton jump diffusion processes

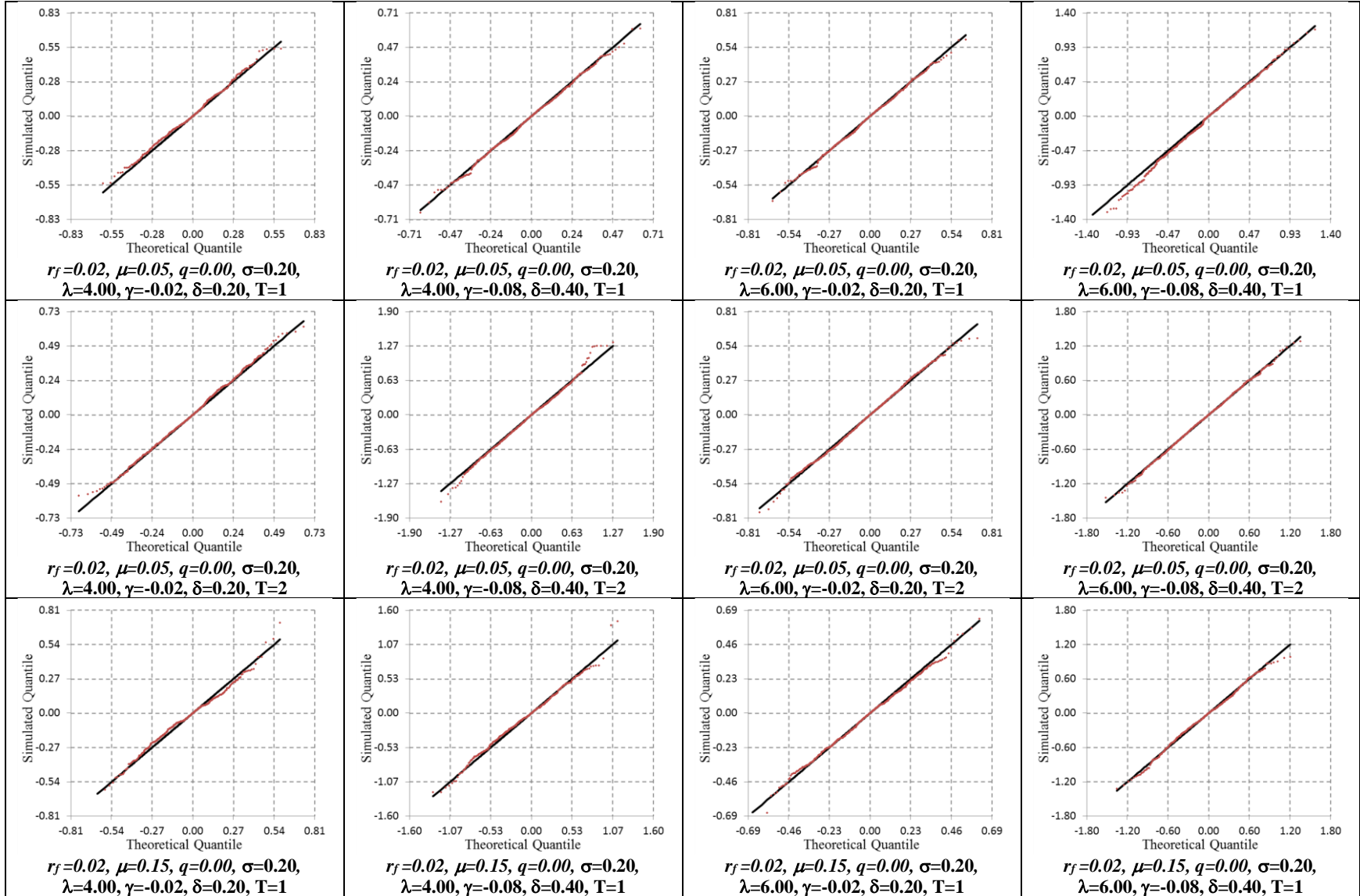
r_f	μ	q	σ	λ	δ	T	Exp. Sample Mean Return	Exp. Sample Standard Error	Theo. Mean Return	z-test and t-test statistics	z-test p-value	t-test p-value
2%	5%	0%	20%	400%	20%	1	-8.92E-04	2.05E-06	-8.93E-04	0.304	76%	76%
2%	5%	0%	20%	600%	20%	1	-1.34E-03	2.69E-06	-1.34E-03	0.551	58%	59%
2%	5%	0%	20%	400%	40%	1	-3.57E-03	7.52E-06	-3.57E-03	0.528	60%	60%
2%	5%	0%	20%	600%	40%	1	-5.35E-03	9.79E-06	-5.35E-03	0.066	95%	95%
2%	15%	0%	20%	400%	20%	1	-9.22E-04	1.65E-06	-9.23E-04	0.750	45%	46%
2%	15%	0%	20%	600%	20%	1	-1.36E-03	2.63E-06	-1.36E-03	0.290	77%	77%
2%	15%	0%	20%	400%	40%	1	-3.63E-03	5.83E-06	-3.64E-03	1.470	14%	15%
2%	15%	0%	20%	600%	40%	1	-5.42E-03	9.51E-06	-5.41E-03	0.772	44%	45%
2%	5%	0%	20%	400%	20%	2	-1.78E-03	2.54E-06	-1.79E-03	0.965	33%	34%
2%	5%	0%	20%	600%	20%	2	-2.67E-03	3.17E-06	-2.67E-03	0.068	95%	95%
2%	5%	0%	20%	400%	40%	2	-7.15E-03	9.05E-06	-7.14E-03	0.970	33%	34%
2%	5%	0%	20%	600%	40%	2	-1.07E-02	1.13E-05	-1.07E-02	0.315	75%	76%
2%	15%	0%	20%	400%	20%	2	-1.84E-03	3.02E-06	-1.85E-03	0.359	72%	72%
2%	15%	0%	20%	600%	20%	2	-2.73E-03	2.77E-06	-2.73E-03	0.097	92%	92%
2%	15%	0%	20%	400%	40%	2	-7.28E-03	1.27E-05	-7.28E-03	0.096	92%	92%
2%	15%	0%	20%	600%	40%	2	-1.08E-02	1.17E-05	-1.08E-02	0.092	93%	93%
8%	20%	5%	40%	400%	20%	1	-1.46E-03	2.06E-06	-1.46E-03	0.508	61%	62%
8%	20%	5%	40%	800%	20%	1	-2.35E-03	2.42E-06	-2.35E-03	1.312	19%	20%
8%	20%	5%	40%	400%	40%	1	-4.17E-03	1.00E-05	-4.17E-03	0.542	59%	59%
8%	20%	5%	40%	800%	40%	1	-7.73E-03	1.07E-05	-7.73E-03	0.098	92%	92%
r_f = riskless rate of interest; μ = diffusion statistical drift; σ = diffusion volatility; q = dividend yield; λ = arrival rate of jumps (per year); $\gamma = -\delta^2/2$ = jump amplitude; δ = volatility of jump amplitude; T = simulation horizon (years) Experiment parameters: time step number = 90; simulation number = 50,000; resampling pooling = 10; resampling simulation number = 10,000												

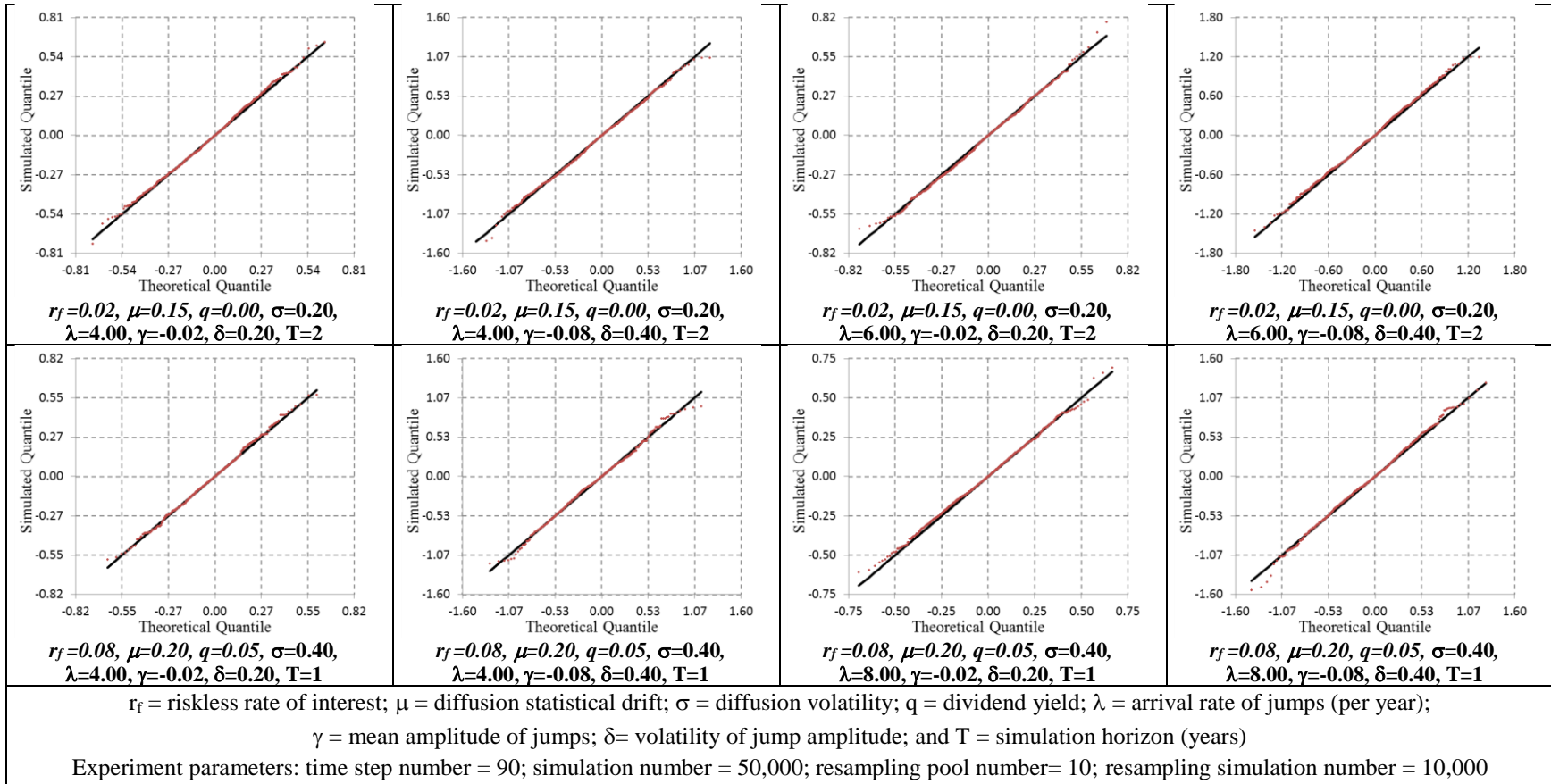
ANNEX D.1: Q-Q plots for the distributions induced by combined simulations, non-parametric Esscher transforms, and bootstrap of geometric Brownian motions





ANNEX D.2: Q-Q plots for the distributions induced by combined simulations, non-parametric Esscher transforms and bootstrap of jump-diffusion processes





ANNEX E.1: Kolmogorov-Smirnov tests for the distributions induced by combined simulations, non-parametric Esscher transforms, and resampling of twenty cases of geometric Brownian motions

r_f	μ	q	σ	T	Kolmogorov Smirnov statistic	p -value
2.0%	5%	0%	20%	1.0	0.813	52%
2.0%	20%	0%	20%	1.0	0.877	43%
2.0%	5%	0%	40%	1.0	0.594	87%
2.0%	20%	0%	40%	1.0	0.827	50%
8.0%	5%	0%	20%	1.0	0.700	71%
8.0%	20%	0%	20%	1.0	0.580	89%
8.0%	5%	0%	40%	1.0	0.700	71%
8.0%	20%	0%	40%	1.0	0.453	99%
2.0%	5%	0%	20%	2.0	0.870	44%
2.0%	20%	0%	20%	2.0	0.919	37%
2.0%	5%	0%	40%	2.0	1.223	10%
2.0%	20%	0%	40%	2.0	1.216	10%
8.0%	5%	0%	20%	2.0	0.735	65%
8.0%	20%	0%	20%	2.0	1.181	12%
8.0%	5%	0%	40%	2.0	0.679	75%
8.0%	20%	0%	40%	2.0	1.089	19%
2.0%	5%	5%	20%	1.0	1.110	17%
2.0%	20%	5%	20%	1.0	0.976	30%
2.0%	5%	15%	20%	1.0	1.131	15%
2.0%	20%	15%	20%	1.0	0.566	91%
r_f = riskless rate of interest; μ = diffusion statistical drift; σ = diffusion volatility; q = dividend yield; T = simulation horizon (years) Experiment parameters: time step number = 90; simulation number = 80,000; resampling pooling = 4; resampling simulation number = 20,000						

ANNEX E.2: Kolmogorov-Smirnov tests for the distributions induced by combined simulations, non-parametric Esscher transforms, and resampling of twenty cases of Merton jump-diffusion process

r_f	μ	q	σ	λ	δ	T	Kolmogorov Smirnov statistic	p -value
2.0%	5%	0.0%	20%	400%	20%	1.0	1.010	26%
2.0%	5%	0.0%	20%	600%	20%	1.0	0.790	56%
2.0%	5%	0.0%	20%	400%	40%	1.0	0.780	58%
2.0%	5%	0.0%	20%	600%	40%	1.0	0.660	78%
2.0%	15%	0.0%	20%	400%	20%	1.0	0.630	82%
2.0%	15%	0.0%	20%	600%	20%	1.0	0.850	47%
2.0%	15%	0.0%	20%	400%	40%	1.0	0.650	79%
2.0%	15%	0.0%	20%	600%	40%	1.0	1.060	21%
2.0%	5%	0.0%	20%	400%	20%	2.0	0.930	35%
2.0%	5%	0.0%	20%	600%	20%	2.0	0.910	38%
2.0%	5%	0.0%	20%	400%	40%	2.0	0.750	63%
2.0%	5%	0.0%	20%	600%	40%	2.0	1.080	19%
2.0%	15%	0.0%	20%	400%	20%	2.0	0.740	64%
2.0%	15%	0.0%	20%	600%	20%	2.0	1.100	18%
2.0%	15%	0.0%	20%	400%	40%	2.0	0.700	71%
2.0%	15%	0.0%	20%	600%	40%	2.0	0.680	74%
8.0%	20%	5.0%	40%	400%	20%	1.0	0.620	84%
8.0%	20%	5.0%	40%	800%	20%	1.0	0.640	81%
8.0%	20%	5.0%	40%	400%	40%	1.0	1.060	21%
8.0%	20%	5.0%	40%	800%	40%	1.0	0.990	28%
r_f = riskless rate of interest; μ = diffusion statistical drift; σ = diffusion volatility; q = dividend yield; λ = arrival rate of jumps (per year); $\gamma = -\delta^2/2$ = jump amplitude; δ = volatility of jump amplitude; T = simulation horizon (years) Experiment parameters: time step number = 90; simulation number = 50,000; resampling pooling = 10; resampling simulation number = 10,000								

ANNEX F.1: Mean of the distribution induced by combined simulation, non-parametric Esscher transforms, and resampling of twenty cases of geometric Brownian motions

r_f	μ	q	σ	T	Experimental Sample Mean Return	Experimental Sample Standard Error	Theoretical Mean Return	z-test and t-test statistic	z-test p-value	t-test p-value
2%	5%	0%	20%	1	-4.34E-05	2.75E-05	-3.85E-20	1.579	11%	13%
2%	20%	0%	20%	1	2.24E-05	3.33E-05	-3.85E-20	0.674	50%	51%
2%	5%	0%	40%	1	-6.60E-04	4.98E-05	-6.67E-04	0.135	89%	89%
2%	20%	0%	40%	1	-7.08E-04	5.58E-05	-6.67E-04	0.750	45%	46%
8%	5%	0%	20%	1	6.72E-04	2.97E-05	6.67E-04	0.173	86%	86%
8%	20%	0%	20%	1	6.89E-04	2.29E-05	6.67E-04	0.974	33%	34%
8%	5%	0%	40%	1	-6.59E-05	5.02E-05	-1.54E-19	1.314	19%	20%
8%	20%	0%	40%	1	-9.56E-05	7.28E-05	-1.54E-19	1.315	19%	20%
2%	5%	0%	20%	2	3.59E-05	4.77E-05	-7.71E-20	0.752	45%	46%
2%	20%	0%	20%	2	2.94E-05	3.51E-05	-7.71E-20	0.837	40%	41%
2%	5%	0%	40%	2	-1.36E-03	8.63E-05	-1.33E-03	0.271	79%	79%
2%	20%	0%	40%	2	-1.30E-03	7.95E-05	-1.33E-03	0.442	66%	66%
8%	5%	0%	20%	2	1.27E-03	3.87E-05	1.33E-03	1.760	8%	9%
8%	20%	0%	20%	2	1.37E-03	3.34E-05	1.33E-03	0.985	32%	33%
8%	5%	0%	40%	2	-4.90E-05	7.41E-05	-3.08E-19	0.661	51%	51%
8%	20%	0%	40%	2	4.49E-05	7.28E-05	-3.08E-19	0.617	54%	54%
2%	5%	5%	20%	1	-5.66E-04	3.05E-05	-5.56E-04	0.339	73%	74%
2%	20%	5%	20%	1	-5.58E-04	3.02E-05	-5.56E-04	0.067	95%	95%
2%	5%	15%	20%	1	-1.71E-03	3.38E-05	-1.67E-03	1.385	17%	18%
2%	20%	15%	20%	1	-1.67E-03	3.45E-05	-1.67E-03	0.095	92%	93%

r_f = riskless rate of interest; μ = diffusion statistical drift; σ = diffusion volatility;
 q = dividend yield; T = simulation horizon (years)
 Experiment parameters: time step number = 90; simulation number = 80,000;
 resampling pooling = 4; resampling simulation number = 20,000

ANNEX F.2: Mean of the distribution induced by combined simulation, non-parametric Esscher transforms, and resampling of twenty cases of Merton jump diffusion processes

r_f	μ	q	σ	λ	δ	T	Exp. Sample Mean Return	Exp. Sample Standard Error	Theo. Mean Return	t -test and z -test statistics	z -test p -value	t -test p -value
2%	5%	0%	20%	400%	20%	1	-9.03E-04	2.31E-05	-8.93E-04	0.434	66%	67%
2%	5%	0%	20%	600%	20%	1	-1.38E-03	3.46E-05	-1.34E-03	1.217	22%	23%
2%	5%	0%	20%	400%	40%	1	-3.57E-03	5.32E-05	-3.57E-03	0.066	95%	95%
2%	5%	0%	20%	600%	40%	1	-5.38E-03	5.97E-05	-5.35E-03	0.509	61%	61%
2%	15%	0%	20%	400%	20%	1	-9.26E-04	2.41E-05	-9.23E-04	0.107	92%	92%
2%	15%	0%	20%	600%	20%	1	-1.37E-03	3.12E-05	-1.36E-03	0.218	83%	83%
2%	15%	0%	20%	400%	40%	1	-3.63E-03	5.71E-05	-3.64E-03	0.197	84%	84%
2%	15%	0%	20%	600%	40%	1	-5.47E-03	3.77E-05	-5.41E-03	1.657	10%	11%
2%	5%	0%	20%	400%	20%	2	-1.78E-03	3.35E-05	-1.79E-03	0.242	81%	81%
2%	5%	0%	20%	600%	20%	2	-2.75E-03	4.66E-05	-2.67E-03	1.641	10%	11%
2%	5%	0%	20%	400%	40%	2	-7.21E-03	7.41E-05	-7.14E-03	0.939	35%	36%
2%	5%	0%	20%	600%	40%	2	-1.06E-02	8.96E-05	-1.07E-02	1.281	20%	21%
2%	15%	0%	20%	400%	20%	2	-1.88E-03	3.97E-05	-1.85E-03	0.852	39%	40%
2%	15%	0%	20%	600%	20%	2	-2.78E-03	3.69E-05	-2.73E-03	1.551	12%	13%
2%	15%	0%	20%	400%	40%	2	-7.21E-03	8.28E-05	-7.28E-03	0.854	39%	40%
2%	15%	0%	20%	600%	40%	2	-1.07E-02	7.84E-05	-1.08E-02	1.347	18%	19%
8%	20%	5%	40%	400%	20%	1	-1.41E-03	3.56E-05	-1.46E-03	1.275	20%	21%
8%	20%	5%	40%	800%	20%	1	-2.34E-03	4.02E-05	-2.35E-03	0.201	84%	84%
8%	20%	5%	40%	400%	40%	1	-4.08E-03	5.44E-05	-4.17E-03	1.751	8%	9%
8%	20%	5%	40%	800%	40%	1	-7.64E-03	5.18E-05	-7.73E-03	1.605	11%	12%
<p>r_f = riskless rate of interest; μ = diffusion statistical drift; σ = diffusion volatility; q = dividend yield; λ = arrival rate of jumps (per year); $\gamma = -\delta^2/2$ = jump amplitude; δ = volatility of jump amplitude; T = simulation horizon (years) Experiment parameters: time step number = 90; simulation number = 50,000; resampling pooling = 10; resampling simulation number = 10,000</p>												

ANNEX G: Trigger boundary positions for geometric Brownian motions

Comparison		Trigger Boundary Position with respect to Finite Difference Method			
Option Parameters	Spot Price	RMSE	Max. Relative Error	Initial Relative Error (T_0)	Hausdorff Distance
$\mu=0.05, r=0.02,$ $q=0.05, K=1,$ $\sigma=0.20, T=1.0$	0.8	0.0142	1.4%	1.4%	0.0182
	0.9	0.0153	2.0%	2.0%	0.0256
	1	0.0200	2.4%	2.4%	0.0305
	1.1	0.0174	1.8%	1.4%	0.0215
	1.2	0.0217	2.1%	2.0%	0.0260
$\mu =0.20, r=0.02,$ $q=0.05, K=1,$ $\sigma=0.20, T=1.0$	0.8	0.0150	1.6%	1.4%	0.0177
	0.9	0.0231	2.4%	2.4%	0.0311
	1	0.0143	1.8%	0.9%	0.0194
	1.1	0.0143	1.5%	1.3%	0.0170
	1.2	0.0172	1.7%	1.7%	0.0214
$\mu =0.05, r=0.02,$ $q=0.05, K=1,$ $\sigma=0.40, T=1.0$	0.8	0.0522	4.2%	2.9%	0.0522
	0.9	0.0616	5.6%	5.4%	0.0967
	1	0.0458	3.7%	3.6%	0.0635
	1.1	0.0384	3.5%	1.9%	0.0375
	1.2	0.0585	6.2%	1.0%	0.0653
$\mu =0.20, r=0.02,$ $q=0.05, K=1,$ $\sigma=0.40, T=1.0$	0.8	0.0375	3.0%	2.0%	0.0371
	0.9	0.0371	3.2%	3.1%	0.0542
	1	0.0555	3.9%	3.5%	0.0619
	1.1	0.0455	3.6%	3.1%	0.0553
	1.2	0.0599	4.7%	3.3%	0.0589
r_f = riskless rate of interest; μ = diffusion statistical drift; σ = diffusion volatility; q = dividend yield; K = strike price; T = simulation horizon (years) Experiment parameters: time step number = 180; simulation number = 50,000; resampling pooling = 4; ; resampling simulation number = 50,000					

ANNEX H.1: European and American option prices computed by combined simulations, non-parametric Esscher transforms, and resampling of geometric Brownian motions

Comparison		European Call Option			American Call Option			
Option Parameters	Spot Price	Black-Scholes Method	Non Parametric Method	Diff.	Finite Difference Method	Non Parametric Method	Diff.	Expected Time to Hit Trigger
$\mu=0.05, r=0.02,$ $q=0.05, K=1,$ $\sigma=0.20, T=1.0$	0.8	0.0084	0.0084	0.8%	0.0087	0.0087	0.2%	0.91
	0.9	0.0271	0.0273	0.6%	0.0282	0.0280	-0.6%	0.85
	1	0.0633	0.0633	0.0%	0.0665	0.0665	-0.1%	0.74
	1.1	0.1180	0.1181	0.1%	0.1261	0.1259	-0.1%	0.58
$\mu =0.20, r=0.02,$ $q=0.05, K=1,$ $\sigma=0.20, T=1.0$	1.2	0.1884	0.1883	-0.1%	0.2050	0.2047	-0.2%	0.35
	0.8	0.0084	0.0084	-0.9%	0.0087	0.0086	-0.7%	0.88
	0.9	0.0271	0.0274	0.9%	0.0282	0.0284	0.8%	0.80
	1	0.0633	0.0634	0.2%	0.0665	0.0665	0.0%	0.68
$\mu =0.05, r=0.02,$ $q=0.05, K=1,$ $\sigma=0.40, T=1.0$	1.1	0.1180	0.1183	0.2%	0.1261	0.1263	0.2%	0.51
	1.2	0.1884	0.1884	0.0%	0.2050	0.2048	-0.1%	0.30
	0.8	0.0546	0.0549	0.6%	0.0556	0.0562	1.1%	0.89
	0.9	0.0916	0.0909	-0.8%	0.0937	0.0932	-0.5%	0.85
$\mu =0.20, r=0.02,$ $q=0.05, K=1,$ $\sigma=0.40, T=1.0$	1	0.1390	0.1384	-0.5%	0.1426	0.1421	-0.4%	0.81
	1.1	0.1958	0.1963	0.3%	0.2017	0.2008	-0.5%	0.76
	1.2	0.2607	0.2600	-0.3%	0.2696	0.2684	-0.5%	0.69
	0.8	0.0546	0.0547	0.1%	0.0556	0.0557	0.1%	0.88
$\mu =0.20, r=0.02,$ $q=0.05, K=1,$ $\sigma=0.40, T=1.0$	0.9	0.0916	0.0918	0.1%	0.0937	0.0940	0.4%	0.84
	1	0.1390	0.1397	0.5%	0.1426	0.1430	0.2%	0.79
	1.1	0.1958	0.1964	0.1%	0.2017	0.2019	0.1%	0.73
	1.2	0.2607	0.2602	-0.2%	0.2696	0.2687	-0.4%	0.66

r_f = riskless rate of interest; μ = diffusion statistical drift; σ = diffusion volatility;
 q = dividend yield; K = strike price; T = simulation horizon (years)
 Experiment parameters: time step number = 180; simulation number = 50,000;
 resampling pooling = 4; ; resampling simulation number = 50,000

ANNEX H.2: European and American option prices computed by combined simulations, non-parametric Esscher transforms, and resampling of Merton jump-diffusion processes

Comparison		European Call Option			American Call Option	
Option Parameters	Spot Price	Esscher Adjusted Merton Model	Non Parametric Method	Diff.	Non Parametric Method	Expected Time to Hit Trigger
$\mu = 0.05, r=0.02,$ $q=0.05, K=1,$ $\sigma=0.20, \lambda = 1.00,$ $\gamma = -\delta^2/2 ; \delta=0.20,$ $T=1.00$	0.8	0.0237	0.0236	-0.1%	0.0240	0.91
	0.9	0.0503	0.0503	0.1%	0.0515	0.88
	1	0.0916	0.0917	0.0%	0.0944	0.83
	1.1	0.1475	0.1476	0.1%	0.1525	0.75
	1.2	0.2155	0.2156	0.1%	0.2247	0.64
$\mu = 0.05, r=0.02,$ $q=0.05, K=1,$ $\sigma=0.20, \lambda = 1.00,$ $\gamma = -\delta^2/2 ; \delta=0.40,$ $T=1.0$	0.8	0.0600	0.0621	3.4%	0.0629	0.91
	0.9	0.0949	0.0971	0.1%	0.0986	0.91
	1	0.1418	0.1440	1.5%	0.1459	0.90
	1.1	0.2003	0.2021	0.9%	0.2052	0.89
	1.2	0.2682	0.2695	0.5%	0.2739	0.87
$\mu = 0.05, r=0.02,$ $q=0.05, K=1,$ $\sigma=0.20, \lambda = 2.00,$ $\gamma = -\delta^2/2 ; \delta=0.20,$ $T=1.0$	0.8	0.0386	0.0386	-0.1%	0.0392	0.91
	0.9	0.0705	0.0704	-0.1%	0.0719	0.89
	1	0.1151	0.1150	-0.1%	0.1174	0.85
	1.1	0.1715	0.1714	0.0%	0.1758	0.80
	1.2	0.2380	0.2380	0.0%	0.2451	0.73
$\mu = 0.05, r=0.02,$ $q=0.05, K=1,$ $\sigma=0.20, \lambda = 2.00,$ $\gamma = -\delta^2/2 ; \delta=0.40,$ $T=1.0$	0.8	0.1040	0.1053	1.2%	0.1063	0.93
	0.9	0.1475	0.1488	0.9%	0.1505	0.92
	1	0.1997	0.2009	0.6%	0.2037	0.90
	1.1	0.2599	0.2609	0.4%	0.2651	0.89
	1.2	0.3267	0.3276	0.3%	0.3331	0.87
$\mu = 0.20, r=0.02,$ $q=0.05, K=1,$ $\sigma=0.20, \lambda = 1.00,$ $\gamma = -\delta^2/2 ; \delta=0.20,$ $T=1.0$	0.8	0.0244	0.0246	0.7%	0.0248	0.94
	0.9	0.0537	0.0539	0.4%	0.0547	0.91
	1	0.0983	0.0983	0.0%	0.0998	0.85
	1.1	0.1565	0.1563	-0.1%	0.1596	0.78
	1.2	0.2256	0.2253	-0.2%	0.2318	0.66
$\mu = 0.20, r=0.02,$ $q=0.05, K=1,$ $\sigma=0.20, \lambda = 1.00,$ $\gamma = -\delta^2/2 ; \delta=0.40,$ $T=1.0$	0.8	0.0599	0.0606	1.1%	0.0613	0.96
	0.9	0.1005	0.1011	0.6%	0.1021	0.95
	1	0.1538	0.1541	0.2%	0.1557	0.94
	1.1	0.2173	0.2172	-0.1%	0.2194	0.93
	1.2	0.2882	0.2877	-0.2%	0.2908	0.91
$\mu = 0.20, r=0.02,$ $q=0.05, K=1,$ $\sigma=0.20, \lambda = 2.00,$ $\gamma = -\delta^2/2 ; \delta=0.20,$ $T=1.0$	0.8	0.0391	0.0389	-0.4%	0.0391	0.94
	0.9	0.0732	0.0735	0.5%	0.0740	0.92
	1	0.1202	0.1204	0.1%	0.1220	0.88
	1.1	0.1787	0.1787	0.0%	0.1818	0.83
	1.2	0.2463	0.2461	-0.1%	0.2515	0.76
$\mu = 0.20, r=0.02,$ $q=0.05, K=1,$ $\sigma=0.20, \lambda = 2.00,$ $\gamma = -\delta^2/2 ; \delta=0.40,$ $T=1.0$	0.8	0.1036	0.1032	-0.4%	0.1040	0.95
	0.9	0.1502	0.1497	-0.4%	0.1510	0.94
	1	0.2059	0.2054	-0.3%	0.2073	0.93
	1.1	0.2690	0.2684	-0.2%	0.2712	0.91
	1.2	0.3378	0.3373	-0.2%	0.3412	0.89

r_f = riskless rate of interest; μ = diffusion statistical drift; σ = diffusion volatility; q = dividend yield;
 λ = arrival rate of jumps (per year); $\gamma = -\delta^2/2$ = jump amplitude; δ = volatility of jump amplitude;
 K = strike price; T = simulation horizon (years)

Experiment parameters: time step number = 180; simulation number = 50,000;
resampling pooling = 4; resampling simulation number = 50,000